Transport Metropolitan Optical Networking: Evolving Trends in the Architecture Design and Computer Modeling

N. Antoniades, *Member, IEEE*, I. Roudas, G. Ellinas, *Member, IEEE*, and J. Amin

***Abstract*—This paper presents our work on the design, engineering, and evaluation of end-to-end performance of circuit-switched, wavelength-division multiplexed, optical regional metropolitan area networks. From our initial research efforts on studying and quantifying the benefits of optical transparency in metropolitan area networks, to identifying the key transport-layer transmission impairments which affect the performance of these networks, to a semianalytic technique used for engineering their performance, this paper reviews our work on the subject through several network case studies and clearly demonstrates the architecture evolution trends during the last few years. The second part of the paper presents our current work on the impacts of the network deployment slowdown on the advancement of WDM in metro and in particular the important tradeoffs of performance and cost. A case study of a current metropolitan network implementation is analyzed and the performance of new technologies presented.**

***Index Terms*—Architecture design, engineering, metro WDM networks, simulation.**

I. Introduction

SINCE the adoption of the SONET/SDH standard, the architectures of optical metropolitan area networks (MANs) have constantly evolved. The predicted exponential increase in data traffic led to the introduction of wavelength division multiplexing (WDM) in optical MANs, as a means for cost-effective capacity upgrade. Early research efforts in this direction (e.g., RACE/ACTS [1] and DARPA-funded [2]–[4] consortia projects) proposed a number of optical multiwavelength network elements (e.g., optical add/drop multiplexers (OADMs), optical cross connects (OXCs)], which were designed to account for the technological constraints of that time period [e.g., small number of wavelengths, large channel spacing, limited selection of WDM components, etc.) and that promoted the concept of network transparency [5]. Over the past few years, these constraints were partially alleviated due to the dramatic improvements in WDM component technology, and the original network element designs went through a succession of transformations [6], [7]. The commercial sector's interest in the subject grew and a number of studies were performed to investigate the feasibility of transparency on the optical layer [8]–[20]. These theoretical studies served as the springboard for the first metro network element prototypes that started being developed in the commercial sector's optical networking laboratories and deployed in field-trial implementations [21]–[30].

In parallel, the first commercial WDM metro network elements entered the regional metropolitan area network space [31], [32], [46]. At the same time architectures started moving forward with new concepts like Broadcast & Select (B&S), which at their introductory phase seemed to apply only for the long-haul part of the network [33], but eventually started seeing implementations (or rather suggested applications) in the metropolitan area as well [34]. The development of analytical/numerical models and commercial software products for computer-aided design of optical MANs followed a parallel evolution. A number of commercial software packages have been developed that deal with the multiple-layer simulation of optical communication networks [35]–[37]. All of them have detail simulation models that can be used to engineer and design MANs. They have the capability to model the more important performance impairments of the optical transport layer that transparency imposes on such systems and networks.

Recent theoretical [9] and experimental [38] results indicate that, in the envisioned all-optical MAN architectures, the most significant transmission impairments are, in order of decreasing importance, the optical amplifier related effects (i.e., optical power ripple, optical signal-to-noise ratio (SNR) divergence, amplified spontaneous emission (ASE) noise accumulation, and optical power transients), the signal distortion due to chromatic dispersion and its interplay with the transmitter chirp, the signal distortion due to optical multiplexer/demultiplexer (MUX/DMUX) concatenation, mainly in parallel architectures, the linear optical crosstalk, if transparent OXCs are used, the polarization-dependent loss (PDL), the polarization-mode dispersion (PMD), in the case of long links of old legacy fibers, and the fiber nonlinearities, in the case of high bit rates and long distances.

Unfortunately, the introduction of all-optical dense wavelength-division multiplexing (DWDM) equipment and architectures in the metro environment for replacement of the traditional architectures or for any green-field scenarios as initially envisioned has been slowed down significantly by the current economic downturn. As a result, the network architectures that are actually being deployed today require a focus on only a

Manuscript received January 21, 2004; revised June 25, 2004.

N. Antoniades is with the Department of Engineering Science & Physics, The College of Staten Island, The City University of New York, Staten Island, NY 10314 USA (e-mail: antoniades@mail.csi.cuny.edu).

I. Roudas is with the Department of Electrical Engineering, University of Patras, Patras, Greece.

G. Ellinas is with the Electrical Engineering Department, The City College of New York, City University of New York, New York, NY 10031 USA.

J. Amin was with Avanex Inc., Painted Post, NY 14870 USA. He is now with Corning Inc., Corning, NY 14870 USA.

Digital Object Identifier 10.1109/JLT.2004.836776

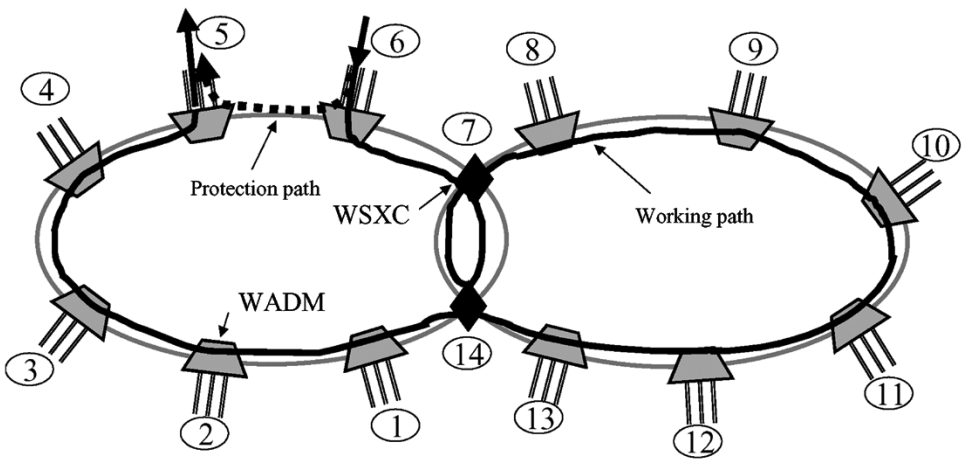

Fig. 1. Metro WDM interconnected-ring simulation case study with examined worst-case path [9].

small number of transport layer impairments rather than the full set that was initially studied since the range of transparency in such designs is still limited. This in a sense has simplified the engineering of such designs. The cost of the components and the design as a whole on the other hand has become extremely important and cost versus performance tradeoffs now play the central role in the design and engineering of metro networks.

This paper starts with a comprehensive review of our work on the design and engineering of regional WDM metropolitan area networks. This sets the stage for our most recent research work on how these networks are designed and engineered today given the very important tradeoff between cost and performance imposed by the current industry conditions. The article starts from our initial efforts on studying and quantifying the benefits of optical transparency in metro (Sections II and III), to identifying the key transport-layer transmission impairments which affect the performance of these networks (Section IV), to a semianalytic technique used for engineering their performance (Section V). In Section VI, several network case studies are presented that clearly present how architectures evolved during the last few years. In Section VII, which presents our latest work, we show that the current telecommunications slowdown had a significant impact on how metro networks are designed and engineered today. It is clear that some major performance impairments which we were concerned with in the past have no significant impact in today's deployed scenarios mainly because the truly transparent paths are much shorter and traverse less components than originally studied. On the center-stage now are the performance versus cost tradeoffs which lead to the use of new and cheap technologies. The current drive is not how far to extend transparent paths but how to make the existing ones work using the simplest and less costly components. A case study of a current metropolitan network implementation is analyzed and the performance of new technologies presented.

II. Network Evolution—The Initial Vision

The infancy of WDM metropolitan area optical networking in the U.S. can be traced back to the early-to-mid-1990s when the various DARPA-funded [2]–[4] consortia were well underway with the first of its kind research studies. Their purpose was to integrate next-generation network architectures, advanced technology, and business drivers to achieve high capacity, high performance, cost effective, reliable, transparent multiwavelength optical networks that met the government demands at the time. The technology applications were intended initially for networks of national scale [4] but eventually were scaled back to metropolitan area-type of designs when certain transparency restrictions became obvious [39]. Clearly, the metropolitan networking environment with its constant and rapidly changing bandwidth requirements, cost sensitivities and nonhomogenous customer traffic needs presented a very unique and difficult application for the deployment of the latest at the time optical technologies. These consortium efforts clearly helped shape and influence the initial industry attempts to understand the limits of transparency, determine its feasibility in the metropolitan environment, quantify its benefits and finally attempt to design and engineer networks in its framework. Fig. 1 presents one of our early attempts to theoretically study transparency in networks of the metropolitan regional size [9]. The architecture was in line with the theoretical research at the time and prototypes such as the Multi-wavelength Optical NETwork (MONET) testbed that was being constructed in Washington, DC [40]. The idea was to investigate transparency employing two interconnected WDM rings with dedicated $(1+1)$ protection, using 32 channels in the range of 1536.609–1561.419 nm with a channel spacing of 100 GHz. The network of Fig. 1 was not based on any realistic network traffic scenario but rather on the initial thoughts that optical nodes need to be connected in rings (following the traditional SONET paradigm) [41] and that possibly different rings could be designed by different vendors and for different application domains but be interconnected in a transparent way [5]. Network nodes of Fig. 1 could be optical add/drop multplexers (OADMs) or the more complicated wavelength selective cross connects (WSXCs). In both cases these network elements were suggested at the time using the traditional parallel architectures (see [9, Figs. 2 and 3]) where all 32 channels were optically demultiplexed switched and then optically multiplexed before they were transmitted on the outgoing fibers. In trying to transparently engineer the network of Fig. 1 for the worst-case path (solid line) it was shown that effects like nonlinearities, power divergence limitations because

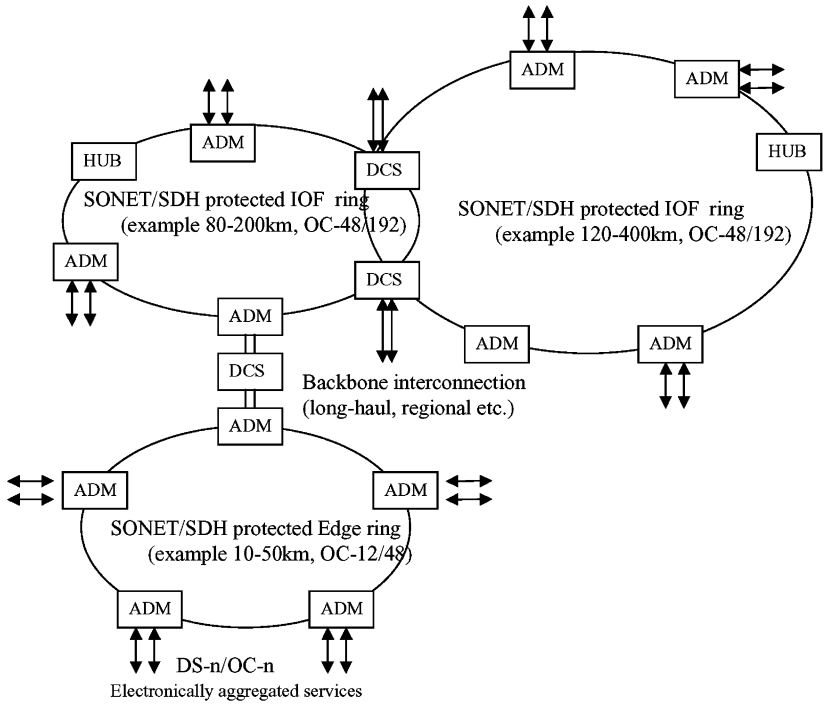

Fig. 2. Current legacy SONET/SDH design in U.S. metropolitan regions [7].

of component imperfections (i.e., ripple) and optical crosstalk were among the most critical. Engineering the network at an exact operating point where all wavelengths would provide sufficient performance [i.e., bit error rate (BER) equal or better than 10^{-12}] proved to be a rather challenging proposition. The tradeoffs between high launched channel power, fiber nonlinearities, and receiver electrical noise were clearly investigated and the boundaries where fiber nonlinearities in metro start becoming important started being drawn. It was also shown that computer modeling and network simulation could be a vital tool for the "virtual engineering" of these network before they are actually deployed. The complexity of doing "complete" (time-domain) network simulations was evident and, although not discussed in detail, the quest for a more efficient semianalytic technique for calculating the performance of such networks was just beginning.

The architecture of Fig. 1 was intended for a green-field metro network case study and naturally the next step was to actually modify it to a more realistic scenario where the new WDM technology would be used to upgrade existing network designs and subsequently investigate transparency-related tradeoffs that were initially touched upon in [9]. The traditional architectures in metro consisted of interconnected fiber SONET/SDH rings as shown in Fig. 2, [7]. In fact, Fig. 2 demonstrates what is still currently the majority of optical networks in North America. On a physical level SONET/SDH is a time-division multiplexing (TDM) frame format which offers bit rate multiplexing capabilities in DS-n or OC-n hierarchical fashion [42]. In Fig. 2 three levels of SONET/SDH ring hierarchy are presented. *Level 1:* The edge rings span distances of a few kilometers to a few tens of kilometers and are composed of add/drop multiplexers (ADMs) that electronically aggregate traffic onto the fiber. Connectivity on these rings is mostly hubbed to a central office location (CO) denoted by a combination of ADMs and digital cross-connect switches (DCSs) on Fig. 2. *Level 2:* DCSs are equipment that interconnect SONET/SDH edge rings to the larger *Inter-OFfice* (IOF) rings that span possibly tens to hundreds kilometers. *Level 3*: IOF rings can also be interconnected using DCSs and can form mesh-connectivity optical networks or larger SONET/SDH rings as shown in Fig. 2.

Clearly, there are three potential routes that can be followed for the expansion of the networks of Fig. 2, namely introducing fiber overlays to deal with any added capacity, the introduction of DWDM that will offer the desired capacity without the need for more fiber (creating new fiber ducts in a metropolitan environment can be a very costly proposition) or a combination of fiber overlays and DWDM. Initial efforts on investigating the feasibility of transparency in metropolitan optical networks focused on transformation of the networks of Fig. 2 into a form of interconnected optical rings as shown in Fig. 3. This type of metro network is comprised of *feeder* (referred to also as IOF or *core*) and *distribution* (referred to also as *collector* or *edge*) sections [6]. The feeder sections aggregate traffic from distribution sections and deliver them to the backbone long-haul network. Edge rings can provide connectivity to individual business or campus-wide networks (shown as buildings in Fig. 3) whereas the feeder section provides the ring-interconnect capability and possible transfer to long-haul backbones without precluding direct customer connections. Typically the feeder sections were envisioned to be based on multiwavelength self-healing rings composed of reconfigurable optical add/drop multiplexers. Ring topologies are preferred due to their efficient fiber sharing and resiliency capabilities [41], [43]. The feeder sections can vary in size, of which the larger ones are referred to as metro *regional*. The distribution sections interface with customer premises, deliver and collect traffic. They can have a

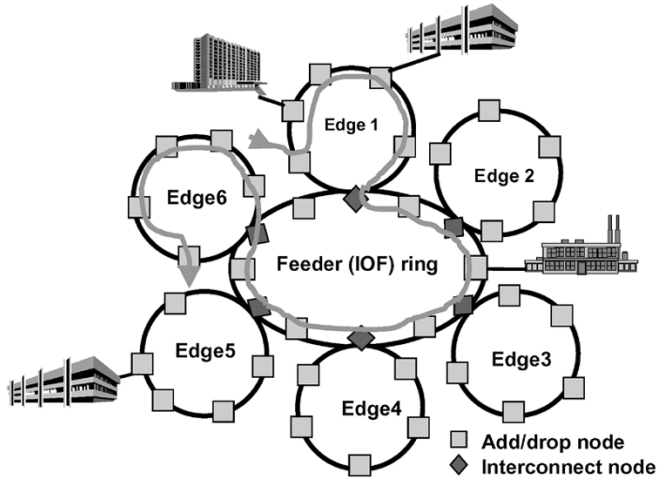

Fig. 3. Typical ring interconnect network architecture used in initial theoretical studies on feasibility of transparency in metro [8]. Add/drop and ring interconnect nodes were envisioned all-optical.

variety of topologies, e.g., tree, bus, single- and double-homed rings, can employ coarse WDM or no WDM and can be totally passive, comprised of low-cost, low-maintenance components. A likely deployment scenario was anticipated to be the introduction of WDM initially into the feeder sections, followed by further penetration into the distribution sections contingent upon the price decrease of WDM components. In addition, it was thought that static OADMs would be deployed in the beginning, with the option for automated (reconfigurable) operation in the future. It must be noted here that Fig. 3 presents the full topology of the WDM network architecture derived as a development of the architecture of Fig. 2 where a hierarchical view of the SONET/SDH architecture is presented. The number of collector rings used in the theoretical studies involving the network of Fig. 3 was chosen at six after typical distances among hubs (ring interconnecting nodes) were defined based on topological design tradeoffs (Section VI). Initial studies focused on the issue of whether the interconnections of the feeder and the distribution rings of Fig. 3 should be done in a transparent or an opaque way. Clearly, the transponders (opaque approach) used at the ring interconnecting nodes of Fig. 3 facilitated network connectivity by providing the benefit of wavelength conversion in addition to the signal conditioning (amplification, power equalization, dispersion compensation) that prevented the accumulation of transport layer performance impairments. However, these transponders were costly and prevented easy network upgrade (i.e., network expansion to accommodate higher bit rates, more customers, etc). Our first theoretical traffic modeling studies on the network of Fig. 3 showed that if transparent ring interconnections were used instead they could provide the same connectivity as the case of opaque ring interconnections; in addition, they could provide the edge over any opaque designs when the cost factor of components and added flexibility in the network (e.g., reconfigurability) are factored in. The above as well as the effects of fiber overlays on the network performance were presented in [8] where extensive traffic modeling was performed using a realistic number of available wavelengths (32) and traffic patterns that included connection deallocation (churn). It was shown that when fiber overlays on the IOF ring are introduced in addition to 32-channel WDM for dealing with increased traffic patterns, provisioning of only one additional fiber overlay significantly reduces blocking (more than 95% call blocking reduction). Two fiber overlays are sufficient to provide the majority of blocking relief. Finally, it was shown in [8] that moderate amounts of churn do not have significant effects on the blocking performance of the metro network of Fig. 3. Clearly, the information derived from the above theoretical studies is very important since it helps network designers avoid costly network overbuilds.

III. Building on the Concepts of Transparency—Network Element Design Evolution

The previous studies confirmed our beliefs that DWDM and all-optical network designs were becoming front-runners for regional metropolitan optical networks. These regional transport rings were thought of as extended versions of the IOF rings of Fig. 3 that could reach circumferences of 400–600 km as suggested in [17] although more typical sizes of about 100–200 km in circumference were considered in most studies. The collector rings are much smaller typically less than 100 km in circumference. An important characteristic of these rings is that they are passive, meaning that in most cases they have no amplifiers or optical switches, so that the design is kept simple, low in maintenance and thus cost effective.

Collector rings are interconnected with the IOF (such as that of Fig. 3) using what are called hub nodes which provide the cross-connect capabilities. However, it is also quite possible that individual customers directly connect to the network through the hubs. Traffic aggregation occurs at either the collector ring or the hub node sites and can involve a wide range of service types such as Internet Protocol (IP), Asynchronous Transfer Mode (ATM), or Frame Relay (FR) over SONET/SDH and Ethernet. Studies like the one in [44] showed that much of the existing traffic demands at the time formed a hubbed connectivity on the collector rings of Fig. 3 meaning that traffic was electronically aggregated at the collector ring nodes and transferred to the hub nodes on individual optical channels from each add/drop site (i.e., edge node-to-hub connectivity). Hub nodes were then used as the aggregation and in some cases the transfer points to the long-haul backbone networks. However, the projections at the time (late 1990s) were that demand for entire wavelength services spanning the collector and IOF rings of the typical metro networks of Fig. 3 was on the rise and in a few years that would be the *de facto* situation in metro [45]. As a result, given the benefits of transparency derived from studies as outlined in Section II above, our research case studies focused on actual design and engineering of network architectures similar to that of Fig. 3, i.e., transparent interconnections of rings at OC-48 and OC-192 bit rates. Some studies and laboratory demonstrations, which will be discussed below, were also performed on single regional metro ring designs (similar to the IOF ring of Fig. 3 but without the feeder ring portions) at both OC-48 (state of the art at the time) and OC-192 and cost-performance tradeoffs were investigated [12], [21].

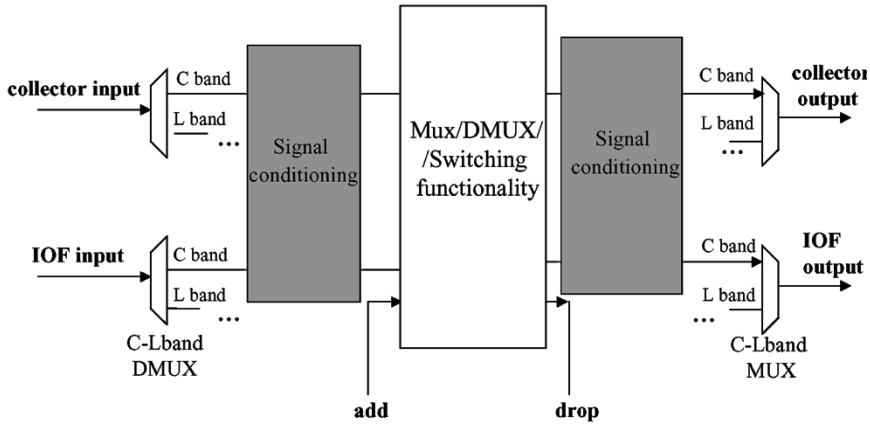

Fig. 4. Typical high-level model implementation diagram of each hub node of Fig. 3 used in some of our modeling case studies.

Initially, the idea of banding and network element designs based on wavelength bands in metro appeared in [6] and was a deviation to the traditional serial or parallel designs used in the earlier projects [4]. As a concept, banding proved to be very important in all our studies (theoretical as well as experimental prototyping) since it allowed for the hierarchical multiplexing/demultiplexing at each collector- or IOF-ring node. The motivation behind banding is that in many cases it is not necessary for every wavelength to be demultiplexed/multiplexed at every node if it carries no traffic for that specific node. As a result, optical node bypassing is a very cost effective solution since: (1) it avoids the use of more expensive demultiplexing equipment and (2) saves on amplification costs since it results in reduced insertion losses on the signal as it passes through all the nodes in its optically transparent path to the destination compared to the case where it had to be demultiplexed and multiplexed several times along the way. In addition, signal distortion due to optical filter concatenation is significantly less due to reduced signal filtering on the worst-case paths. Moreover, allowing for the band-level demultiplexing provides each node with a range of wavelengths over which it can transmit/receive and thus ensures high connectivity within the network design. Our studies, influenced by commercial system realizations at the time such as [46], focused on implementations using 32 channels partitioned into two major bands (C- and L-bands). Each band was then further partitioned into two-to-six other subbands with individual wavelengths spaced 200-GHz apart and a guard spacing between bands. These guard spacings were imposed by limitations of the optical band filtering technologies. The high-level model implementation diagram of each hub node of Fig. 3 used in a subsequent modeling case study analysis is plotted in Fig. 4. It consists of two input and two output fibers corresponding to the collector and IOF ring inputs/outputs. From this figure it is clear that no fiber overlays are assumed; a deviation from the case study of Fig. 3. Studies showed that fiber overlays are very much independent replicas of the basic fiber network design and cases where traffic needs to be interconnected across fiber overlays are rare. The same hub node design of Fig. 4 is repeated for the protection path ($1+1$ protection) and is physically distinct from the working path to avoid single-point of failure scenarios. Our modeling and analytical work on designing and engineering transparent regional metro networks as outlined above was the basis for an experimental effort that actually created a metro network testbed [21]. The actual hub node implementation based on that activity is shown in Fig. 5. The node is essentially a WSXC that first separates the two major bands (C- and L-bands) after having extracted the optical supervisory channel (OSC) which can potentially be used for carrying network management information. For simplicity, only the C-band is drawn in Fig. 5 where Band Pass Filters (BPF1, 2, and 3) drop the desired band in each case and pass through the rest of the bands in a serial fashion. Individual channel MUX/DMUXs are then implemented using multilayer interference filters in a parallel configuration as suggested in [47].

The switching part of the WSXC was assumed as either a simple manual implementation (patch panel) or made of a typical nonblocking switch fabric (for example spanke design) [21]. The signal conditioning functionality of Fig. 4 was achieved with the presence of optical amplifiers, dispersion compensation units and power variable optical attenuators (VOAs). Narrow-band amplifiers specifically designed for the metro space as described in [21] provide individual band amplification while preventing any disruptive spikes in power, resulting from sudden traffic changes, using transient gain control. A dispersion compensation unit can be used on the input side of the IOF ring to deal with any uncompensated dispersion in the IOF ring which represents the longest part of the fiber design. Finally, VOAs on an individual channel basis provide for dynamic power equalization that corrects for any wavelength-dependent loss imperfections in the components. Simplified versions of the WSXC node of Fig. 5 can be used as optical add/drop multiplexers (OADMs) either within the IOF ring or the collector rings of the network topology of Fig. 3. These are simple one-input, one-output network elements which typically employ only one band filter. As a result, if they are used on a typical collector ring each customer (i.e., optical node) gets assigned a waveband for its traffic needs; something advocated in sample commercial product settings [48]. A typical waveband is composed of four channels in our case study of Fig. 3.

As transparency gained significant ground and studies on traffic predictions indicated that from 2000 to 2005 average connection distances in North America would more that quadruple

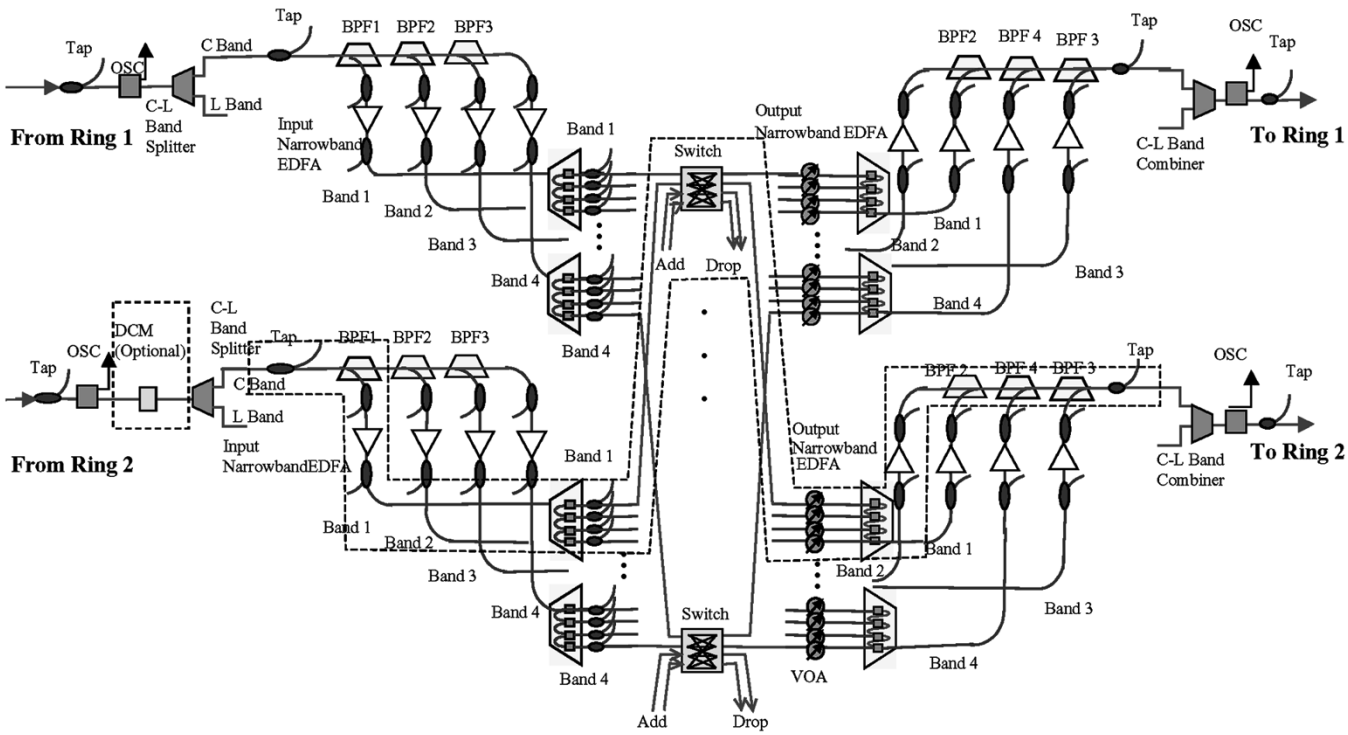

Fig. 5. The full WDM hub node design of the case study of Fig. 3 built for a testbed prototype [21]. The L-band implementation is omitted for simplicity.

[49], it created a new shift in the way network elements were thought and designed. A new OADM architecture called Broadcast and Select (B&S) was proposed in [33] that was designed to tailor to the particular growing needs of data and Internet traffic. At the heart of this new network element architecture shown in Fig. 6 is a wavelength selective device called dynamic spectrum equalizer [50], [51] that can selectively attenuate the power of any passthrough channel, effectively providing the equalizing and blocking functionalities in a single device. All incoming traffic is split into the drop and the passthrough directions using conventional 3-dB splitters. On the drop side power is further split using 1:N passive devices where N is the number of accessing stations. Optical filters can then separate the intended traffic at each station with the possibility of accessing a number of different channels in a dynamic way if the filters are made tunable. The dynamic spectrum equalizer is then used on the passthrough path to block each channel that has been dropped and selected on the first stage as well as equalize all the remaining passthrough and added channels. On the adding side, channels can simply be inserted using a set of N transmitters (tunability is also possible) and N power combiners. Signal conditioning as described before is effectively provided using input/output amplifiers, the dynamic spectrum equalizer and possible dispersion compensators (not shown in Fig. 6). In [33], it was shown that B&S OADMs exhibit exceptionally low channel through loss, offer lower first-installed cost mainly due to the combined capabilities of the dynamic spectrum equalizer and can scale very effectively on an as-needed-basis. B&S seemed to fit very well for applications on the long-haul space mainly due to the fact that in that particular space the majority of the traffic is bypassing the nodes but at the same time potential network reconfigurability

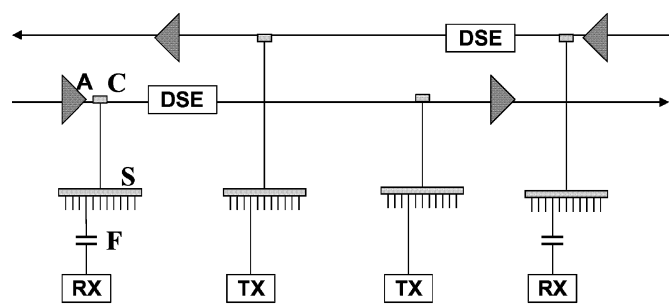

Fig. 6. Typical B&S OADM architecture as proposed in [33]. Figure assumes 1 + 1 protection. F = optical filters, S = 1 to N power splitter, A = optical amplifier, C = 3 dB coupler, DSE = dynamic spectrum equalizer.

at any point calls for capability to access most (or even all) of the channels; a capability that B&S easily provides through the dynamic spectrum equalizer.

Research and development activities in reconfigurable OADMs have increased in intensity over the past few years, primarily for deployment in transparent long haul and ultra long haul networks. However, with the telecom downturn, and the fact that there has been little demand for new long haul networks, much of the recent focus by these reconfigurable OADM vendors has been on reducing the cost of capital for these network elements, and on simplifying their management, thus resulting in a potential reduction in the operational expenses of the network. This, in turn, has led to carriers now considering OADM solutions such as the B&S architecture shown in Fig. 6 as an attractive candidate for next generation metro systems the demand for which, unlike long haul, has continued to grow even through the telecom downturn, albeit at a slow rate [52], [53], [91].

IV. Transport Layer Performance Impairments: Modeling Issues

As aforementioned, numerical simulation is used to assess the feasibility of multiwavelength all-optical network architectures based on competing network element designs and component technologies and compare their performance. In addition, it is used to provide specifications for the network element components. To achieve these goals, it is necessary to accurately and efficiently model key transmission impairments that affect the end-to-end performance of the physical layer of all-optical networks. Over the years, there is an ongoing effort to improve the accuracy and efficiency of the network-oriented models proposed in the literature. The purpose of this section is to present the main impairment models used in our work.

A. Performance Criterion

A characteristic of optical MANs is the existence of fine granularity traffic with a wide range of protocols (e.g., IP, ATM, SONET, GbE, etc.) and modulation formats [6]. Since the performance criteria might vary depending on the modulation format, we consider here the case of digital optical signals with intensity modulation exclusively. In this case, the appropriate performance criterion is the error probability at the output of the direct-detection receiver, even though in practice and in parts of our simulation methodology below the Q factor is commonly used as an alternative for speed and ease of measurement.

For efficiency, it is desirable to semianalytically evaluate the impact of transmission effects on the error probability. As explained later, in several cases it is possible to take into account arbitrary pulse shapes, arbitrary optical and electronic receiver filters, and non-Gaussian photocurrent statistics at the output of the direct-detection receiver.

B. Amplifier-Related Effects

Erbium-doped fiber amplifiers (EDFAs) generate amplified spontaneous emission (ASE) noise. In addition, due to the variation of the transfer function and spontaneous emission factor of EDFAs as a function of wavelength, WDM signals exhibit optical power and optical signal-to-noise ratio (OSNR) divergence. Finally, EDFAs exhibit optical power transients in the case of network reconfiguration, fiber cuts, power loss or equipment failure.

All aforementioned effects might not be a major issue in metro networks with small inter-nodal distances, which typically do not require in-line amplification, and small number of optical network elements (in which case the number of concatenated EDFAs is small). Nevertheless, the magnitude of the above effects can be evaluated using wavelength domain simulation [54]. A number of static or dynamic EDFA models of various degrees of accuracy could be used for this purpose (see, e.g., [55] and the references therein). The role of other components, e.g., servo-controlled variable optical attenuators, on the power budget can be taken into account.

C. Chirp-Induced Penalty

The degradation due to chromatic dispersion from optical MUX/DMUXs and optical fibers is calculated for the worst optical path in the network (as discussed in the next section). For the power levels and distances used in metro, fiber nonlinearities can be usually ignored and the fiber can be modeled as an all-pass filter with quadratic phase, e.g., [56]. The chirp induced penalty can be estimated qualitatively by calculating the amount of eye degradation at the output of the receiver electric low-pass filter [56], [57] or, more accurately, by evaluating the error probability for different receiver types [58]–[61].

Commercially available directly modulated DFB semiconductor lasers exhibit significant variations in their instantaneous power and frequency waveforms between different manufacturers or between different samples of the same manufacturer [61]. A classification of the laser behavior based solely on their transient and adiabatic chirp is proposed in [61]. The instantaneous angular frequency deviation $\dot{\phi}(t)$ of a directly modulated DFB laser is approximately related to its output optical power $P(t)$ through the expression in [62]

$$\dot{\phi}(t) \cong \frac{\alpha}{2}\left[\frac{1}{P(t)}\frac{dP(t)}{dt} + \kappa P(t)\right] \tag{1}$$

where α is the linewidth enhancement factor and κ the adiabatic chirp coefficient. In (1), the first term is called "transient" chirp, and the second term is called "adiabatic" chirp. It is assumed that the output power is sinusoidally modulated as

$$P(t) = P_0(1 + 2m\cos\omega_m t) \tag{2}$$

where P_0 is the transmitted average power, m is the intensity modulation (IM) index, and $f_m = \omega_m/(2\pi)$ is the modulation frequency. This analog waveform can be considered as a special case of a digital waveform composed of alternating ones and zeros, with bit rate equal to $R_b = 2f_m$ and extinction ratio given in [63]

$$(1 + 2m)/(1 - 2m). \tag{3}$$

It can be shown [63] that the eye closure penalty for small IM indexes ($m \ll 1$) is to a first-order approximation with m equal to

$$P_{\text{eye}}^{\text{CD}} = \{[\cos\Phi(\omega_m) - \alpha\sin\Phi(\omega_m)]^2 + h^2\sin^2\Phi(\omega_m)\}^{-\frac{1}{2}}. \tag{4}$$

In (4), $\Phi(\omega_m)$ is the dimensionless parameter defined as

$$\Phi(\omega_m = \pi R_b) = \frac{\pi\lambda^2 R_b^2 DL}{4c} \tag{5}$$

where λ is the carrier wavelength of the transmitted optical waveform, D is the fiber dispersion parameter, L is the fiber length, and c is the velocity of light in vacuum. In (4), h is the frequency modulation (FM) index defined as

$$h = \frac{\kappa\alpha P_0}{\omega_m}. \tag{6}$$

Expression (4) reveals that in the hypothetical case where there is absence of chirp ($\alpha = 0$, transform-limited pulses), only the first term contributes to the eye closure. In this case, for small $\Phi(\omega_m)$, (4) becomes

$$P_{\text{eye}}^{\text{CD}} \cong (1 - \gamma L^2)^{-1} \tag{7}$$

where

$$\gamma = \frac{\pi \lambda^2 R_b^2 D}{4c}. \tag{8}$$

This approximate relationship was given in [64]. In the absence of chirp, there is always penalty independent of the sign of the dispersion parameter D, as expected. In the presence of chirp ($\alpha \neq 0$), the dominant contribution to the penalty is due to transient chirp (second term, proportional to the alpha parameter α). If the alpha parameter α and the dispersion parameter D have opposite signs, the impact of transient chirp is beneficial up to a certain length (i.e., there is pulse compression) and detrimental afterwards. Adiabatic chirp-induced penalty is due to the third term. It is beneficial up to a certain length independent of the sign of the dispersion parameter D.

A phenomenological model which is based on lab measurements of peak-to-peak chirp and chirp duration parameters is presented in [64] and used in some of the case studies below. This simple model describes the chirp/dispersion interactions and their effect on the level of the received 1s and 0s.

D. Optical MUX/DMUX Concatenation

In transparent multiwavelength optical networks, each lightwave signal may be optically multiplexed/demultiplexed several times during propagation from its source to its destination. Optical MUX/DMUXs exhibit nonideal amplitude and phase transfer functions within the optical signal band. That is, their amplitude transfer functions might present passband curvature, tilt, and ripple. In addition, their phase transfer functions might not vary linearly with frequency. These impairments are enhanced when a large number of these devices are cascaded together. Consequently, optical MUX/DMUX concatenation causes signal attenuation and distortion (i.e., intersymbol interference, ISI) and eventually limits the maximum number of optical network elements that can be cascaded.

Signal spectral clipping due to the concatenation of optical MUX/DMUXs introduces an excess loss, which changes the operating point of optical servo-controlled attenuators and EDFAs in the network elements. Therefore, it is necessary to study the interaction between optical MUX/DMUXs, optical servo-controlled attenuators and EDFAs and its impact on the power levels of the optical signal and amplified spontaneous emission (ASE) noise in the network. In addition, it is important to calculate the noise statistics at the output of the direct-detection receiver. The latter can be considered Gaussian for thermal-noise limited receivers but not for the most common case of optically preamplified direct-detection receivers.

All aforementioned effects are included in the model presented in [65]. This comprehensive model is based on a semianalytic technique for the evaluation of the error probability of the network topology. The error probability evaluation takes into account arbitrary pulse shapes, arbitrary optical MUX/DMUX and electronic low-pass filter transfer functions, and non-Gaussian photocurrent statistics at the output of the direct-detection receiver.

E. Incoherent Common-Channel Homodyne Crosstalk

Since the early days of transparent WDM optical communication systems and networks, optical crosstalk was identified as one of the major transmission impairments that can cause severe performance degradation [66]. In current metro networks, the impact of optical crosstalk is anticipated to be small, due to the small size of optical switch fabrics. Nevertheless, it is possible to assess its influence using a number of models with various degrees of accuracy depending on the type of the receiver, e.g., [66], [67].

Optical crosstalk can be distinguished as *common-channel* and *adjacent-channel.* Common-channel crosstalk arises from interference of optical signals of the same nominal wavelength, whereas adjacent-channel crosstalk arises from interference of optical signals of different nominal wavelengths. In optical MANs, common-channel crosstalk is due to nonideal optical multiplexer/demultiplexers (MUX/DMUXs) and optical space switches contained in optical add/drop multiplexers and OXCs. Common-channel crosstalk can be distinguished into *homodyne* and *heterodyne*, depending on whether the optical frequencies of two interferers are the same or not, respectively. A special case of homodyne crosstalk arises when signals originating from the same source and following different paths arrive to the receiver (*multipath homodyne crosstalk*). Multipath homodyne crosstalk terms share the same modulation, but in general, experience different propagation delays, attenuations, phase changes, and polarization changes due to environmental fluctuations. If the optical path length difference between two multipath homodyne crosstalk signals is smaller than the coherence length of the laser, their beating is called *coherent* crosstalk, and otherwise is called *incoherent* crosstalk.

The exact crosstalk penalty in the receiver performance depends on the modulation, frequency, phase, and polarization of the interfering electric fields and the type of the receiver. The power of the interferers can be calculated by wavelength-domain representation [54]. The crosstalk-induced penalty can be evaluated semianalytically using the models by [66], [67]. Different scenarios for the modulation, phase, and polarization of optical signals can be assumed in all aforementioned models.

F. Other Effects

Fiber nonlinearities can be safely assumed negligible for the metropolitan network scenarios discussed in this paper. Previous work has shown that there are cases where fiber nonlinearities can become significant but proper power management reduces their effect [9]. PMD is in general very low for new fibers which are used for the *green-field* metro scenarios discussed in this work so its effect on performance is rather small for bit rates up to OC-192. An analytical model presented in [64] can be used to calculate the dBQ penalty contribution of this effect which typically is of the order of tenths of a dB. PDL-induced ripple can be significant in metro networks where a signal traverses a large number of optical components with no regeneration. This effect can partially be compensated using servo-controlled attenuators which is what

was assumed in all the case studies presented here. A more detail treatment of this effect can be found in [68].

V. Top-Down Integrated Simulation Methodology

Through the network expansion and introduction of new technologies described in this paper, computer modeling and simulation is playing an increasingly important role in providing the ability to perform virtual prototyping and system engineering and testing before the actual network build-up and deployment. Although there are several commercial simulation frameworks and developed software tools for the modeling of telecommunications networks and specifically in the optical networks arena, to our knowledge no product now provides a software tool that is vertically integrated from the physical (transport) layer to the logical and up to the various application layers. Research work in [69] addressed part of the above issue but did not apply a step-by-step methodology on a real network case study.

Our proposed integrated simulation methodology investigates ways to design metropolitan optical networks based on a top-down simulation approach. This is done as follows: the logical and application layers define the physical network topology (connectivity) under consideration. One way of achieving this is based on traffic projections for voice, transaction data, and Internet traffic demands taking into account knowledge of current demands, the change of the population, the change of the nonproduction employees, and the Internet hosts as described in [70]. A model can then be used to impose the above projections onto viable network topologies as shown in [44], [72]. An example of such a derived network topology will be presented in Section VI below. The logical and management layers will then perform the network dimensioning which essentially means assigning the wavelengths and engineering the network. There are two ways of actually doing that: (1) *worst-case engineering*, meaning that we assume the network is populated with maximum number of channels (the word channels and/or wavelengths is used interchangeably here) from day 1 of operation and that all wavelengths have to satisfy transport layer performance requirements on the worst-case paths; (2) engineering based on the *concept of channel yield*, meaning not all channels need to go the entire system length, meaning that we can use the "poor" channels for the shorter connection and the "good" channels for the long distance routes. As a result, only some fraction of channels needs to support maximum reach (typically 80%).

In the first case (worst-case engineering), the interaction of the logical layer with the transport layer is minimal, at least on the design phase of the network, since once the topology is derived from the higher layers and passed on below, the transport layer engineering takes over. During the transport layer engineering phase, all wavelengths need to then be engineered on the worst-case path(s).

In the second case (using the concept of channel yield), a recursive loop is established between the logical and the transport layers. Each service needs to be provisioned and wavelengths need to be assigned to each service (or each group of services). The above simulation methodology is applied on a wavelength-by-wavelength basis and the right wavelength is selected for each service based on its transport layer performance. As a result, the wavelength with the best transport layer performance is assigned for example the longest routes (i.e., worst-case paths if that is the case) whereas the wavelengths with poorer performance are assigned shorter routes. The above represents an innovative way of engineering the performance of such networks and it results in significant cost vs. performance tradeoffs. In a green-field scenario engineering a network using the worst-case approach will require the use of expensive technologies such as state-of-the-art in laser transmitters, optical amplification, dispersion compensation, and component ripple control for all customer services. Clearly, engineering the network using the concept of channel yield will provide significant savings since high performance requirements are now being required from a smaller set of wavelengths (i.e., customers) that might naturally meet those requirements to begin with.

For the remainder of the paper, we concentrate on the worst-case engineering approach. Although the concept of channel yield is clearly more intriguing it requires the interoperability of various network layers which is a subject of our current research work for which results will be presented in the future. Following the above approach, computer simulation can be effectively used for engineering the transport layer of typical metro WDM optical networks, effectively balancing the need for computation accuracy, with speed and topological flexibility. During the last few years, a number of simulation packages intended for the network optical layer have emerged. The operation of the majority of these tools is based on the well-known time- and frequency-domain simulation principles [73].

Unfortunately, simulation of WDM optical communication networks requires a large simulation bandwidth mainly because of the large aggregate bandwidth of the optical signals and the wide range of the ASE noise. Moreover, such networks contain a large number of optical paths over which these time/frequency domain simulations need to be performed. Complete time/frequency domain simulation of metro WDM networks for example is a very time consuming process. As a result, a three-step computationally efficient simulation methodology was introduced in [64] that essentially represents a semianalytic way of performance modeling [73]. The first step involves performing wavelength-domain simulation on the entire network. The wavelength-domain representation that increases speed by increasing resolution bandwidth is presented in great detail in [54]. The approach essentially consists in undersampling the various spectra and ignoring the phase of the signals, which means ignoring their modulation and representing their spectra by simple impulses in the frequency domain. A result of the undersampling performed in wavelength-domain simulation is that switching between time and frequency domains is not possible. The approach is used to calculate the average signal and crosstalk powers and OSNR and not to evaluate the waveform evolution of channels through the optical components of the network. The crosstalk-induced penalties as well as the nonlinear effects in the fiber and other optical components, along with the polarization effects are not captured in the wavelength-domain simulations and are studied only on individual paths of the examined networks in the time-domain simulation part of the approach (step 2). As a result, the time

consuming time/frequency approach is only executed on selected worst-case paths in the network (wavelength-domain simulations and analysis identify these worst-case paths).

The Q factor is used as a convenient and easy to measure and model parameter for system performance. Q is defined in [74] as

$$\mathrm{BER} = \frac{1}{2}\mathrm{erfc}\left(\frac{Q}{\sqrt{2}}\right) \approx \frac{e^{\frac{-Q^2}{2}}}{Q\sqrt{2\pi}}. \tag{9}$$

The Q penalty of a system is often expressed in dB and since we are mostly concerned with the optical penalties introduced by different impairments, we will use the following definition for dBQ throughout the paper: $\mathrm{dBQ} = 10\log(Q_{\mathrm{linear}})$.

The second part of the simulation methodology described earlier can be used to provide the penalties (in dBQ) due to fiber nonlinearities, polarization effects, as well as linear optical crosstalk that cannot be obtained using the wavelength-domain approach of step one. In trying to engineer the performance of an optical network, we need a tool that will be flexible and fast enough to run simulation repetitions for different network parameters, and network sizes so it becomes obvious that repeating steps 1 and 2 above can not effectively help the network designer. A third simulation step is thus introduced that uses information from the previous two steps to determine the Q parameter for the channels on the worst-case path in a simple and time-efficient way. This is a budgeting approach where dBQ penalties for the various effects obtained either from the second step of the simulation methodology presented above or through impairment models are used. The Q performance of all the channels applied on the worst-case path can then be calculated by keeping track of the signal and ASE noise powers starting from the optical transmitter, through the various components and finally at the optical receiver taking into account channel power divergence, dispersion/chirp, ASE noise, receiver noise terms and budgeting for all other impairments in the form of dBQ. It must be noted that this is different from a simplistic Q budget since the margin allocated for each impairment is not a fixed amount, but is calculated from a corresponding impairment model. The main limitation of the above overall approach is the tradeoff of accuracy with speed. During the implementation of the final step (i.e., budgeting analysis on the worst-case path) in trying to do the network engineering certain parameters may change. Ideally then all three steps of the methodology would need to be repeated each time a parameter change occurs increasing the simulation time. In the case studies of Section VI we assumed that parameter changes provide a minimum change in the overall impairment budgeting of the network and thus avoided any iterations. In our latest work in Section VII it is clear that steps 1 and 2 are not needed due to the simplicity of the design and our prior knowledge of effects and thus only budgeting is used.

VI. Design and Engineering of Metro Networks: Case Study Results

In designing metro networks and trying to engineer their performance we use the three-step simulation process outlined in the previous section and employed the models described in detail in Section IV. In this part, we briefly present two simulation case studies before we move on to Section VII where our latest work is presented in more detail.

The difference in the two case studies is the fact that the first focuses on a more theoretical topology that was derived based on the studies on optical transparency described before. The second is a more comprehensive study based on realistic data for a network topology.

The first case study is based on the network architecture of Fig. 3 and focuses on the traced worst-case path (gray line). The optical signal is added on the first node of an edge ring, traverses the whole edge and IOF rings and is dropped at the most distant node of the last edge ring. Besides engineering the performance of the above network, this work dealt with the topology design question of how big a transparent network can we support based on the architecture of Fig. 3. In [64] where the details of the above work is presented, it was shown that we can design each edge ring to consist of a total of 16 km of single-mode fiber and seven nodes spread across that distance. Six hub nodes (i.e., six interconnected edge rings) can be supported each separated by about 15 km bringing the maximum circumference of the IOF ring to about 100 km. Assuming the basic node (hub and edge) design that was prototyped in the lab and shown in Fig. 5 and using simulation parameters derived from experiments [64] the network is engineered for the worst-case at bit rates of OC-48 and OC-192 as shown in Fig. 7. Clearly both cases are engineered successfully for the worst-case paths. Crosstalk plays an important role in this design since the worst-case path goes through a number of optical nodes. Wavelength-domain simulation is used to derive the magnitude of each term and the model described in Section IV applied in part 2 of the simulation procedure is used to derive the 1 dBQ penalty for this effect as described in [64]. Step 2 of the simulation procedure (time-domain) is used to derive the dBQ penalties for the following effects: fiber nonlinearities at 0.1 dBQ and fairly negligible; PDM-induced penalty at 0.1 dBQ again very small; filter concatenation is derived to give a 1 dBQ distortion-induced penalty using DMLs at 2.5 Gb/s whereas EA-modulated and externally modulated transmitters do better (0.5 dBQ). These were derived based on work in [75]. For the results of Fig. 7, EA-modulated transmitters are assumed for the OC-192 case and DMLs for the OC-48 and the phenomenological model for chirp/dispersion in [64] and alluded to in Section IV was used.

The second engineering case study implements the top-down simulation methodology described in Section V to enable a transparent metro network solution of a typical U.S. Incumbent Local Exchange Carrier (ILEC). It uses information consisting of traffic modeling based on projected traffic demands and network dimensioning as shown in [71], [76] to design the topology. Fig. 8 shows a 29-node mesh network based on a carrier's needs in a major U.S. metropolitan region. Wavelength-domain simulation is used to identify the worst-case paths shown in the figure (longest and max number of hops) and to derive the histogram of all crosstalk terms as shown in [76]. Part 2 of our simulation methodology is used to derive the dBQ penalties for all the effects using time-domain simulations on the two paths and the models discussed in Section IV. Fig. 9 shows the error probability as a function of the received OSNR for the case of the optical path with the maximum number of

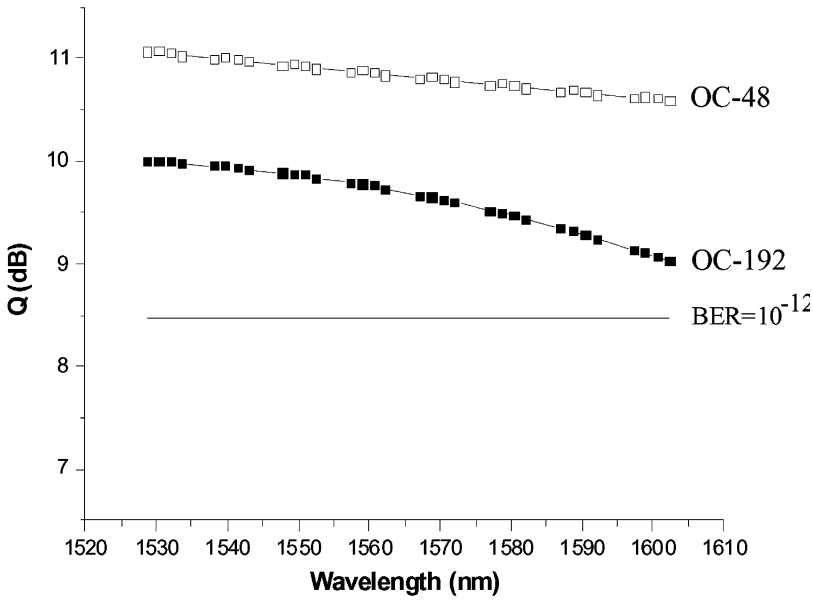

Fig. 7. Q (dB) channel performance for worst-case path of Fig. 3. Results are derived using the three-step simulation procedure of Section V and the models of Section IV. Adequate performance is shown at OC-48 (upper curve) and OC-192 (lower curve) for all channels.

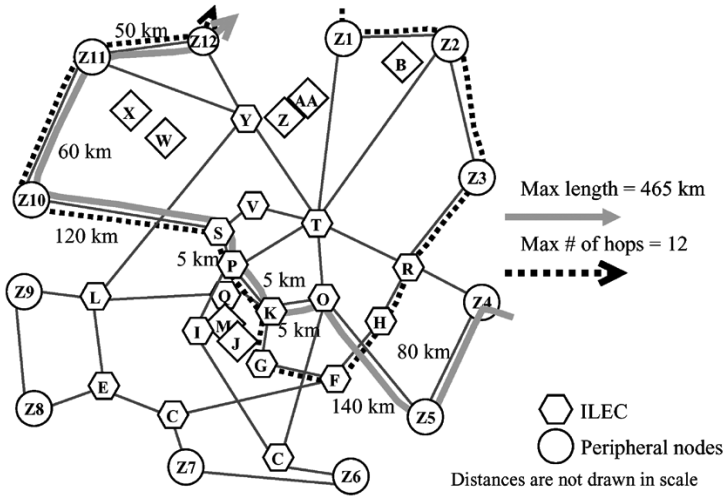

Fig. 8. Metro network case study with identified longest-length path (solid) and maximum number of hops path (dotted). Examined network is that of a carrier and is derived with the top-down simulation approach of Section V, [76].

hops (i.e., worst-case filter concatenation effect). A 0.75-dBQ penalty due to filter concatenation was calculated at a BER of 10^{-12} using the accurate analytical approach outlined in Section IV.

Fiber nonlinearities and polarization effects are further budgeted with 0.5-dBQ penalty. Q budgeting is used as a third and final simulation step in trying to engineer the above network design. In engineering the performance of the network of Fig. 8, we run the above three-step procedure with several iterations until the right configuration of parameters were derived. Amplifier positioning, gain values, resulting black box amplifier noise figure values, and dispersion compensator placements were some of the parameters that we varied during this iterative engineering procedure. Fig. 10 presents the final results of the three-step transport layer simulation methodology. The Q performance of all possible wavelengths for both of the paths examined in Fig. 8 are above the required 8.5 dB (Bit Error Rate $< 10^{-12}$). The shape of the curves is due to the dispersion map of

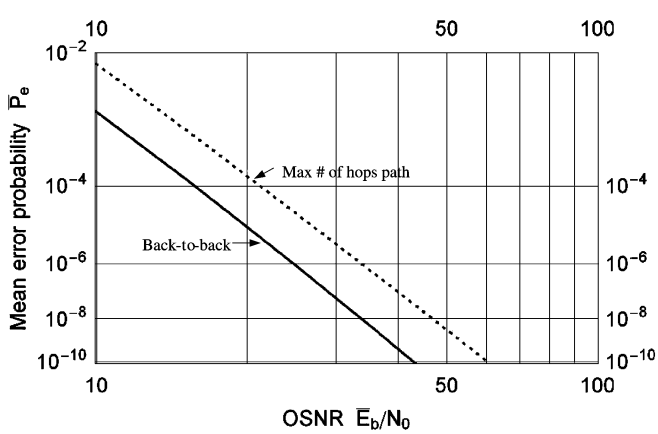

Fig. 9. Mean error probability versus OSNR for the maximum hops path of Fig. 8. Back-to-back (solid) is compared to system with optical filters (dotted).

the system. It is important to note that Fig. 10 demonstrates that engineering for the above worst-case paths assures that 100% of

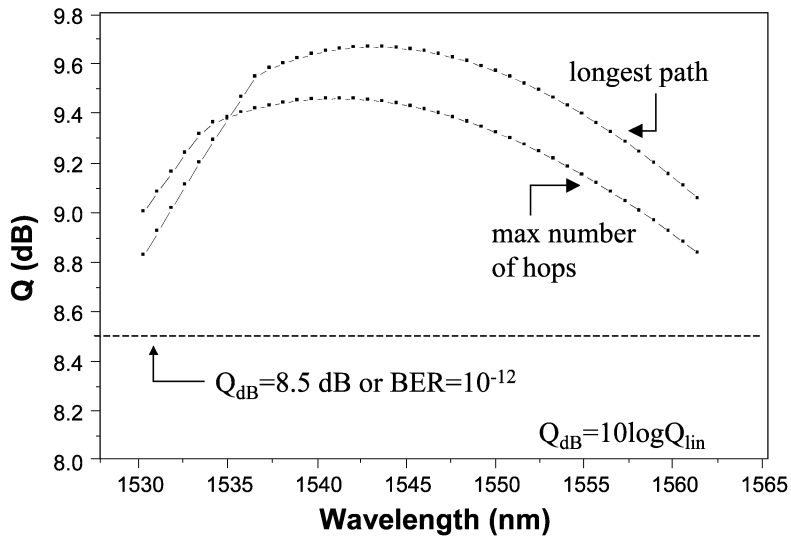

Fig. 10. Q performance results obtained using the Q budgeting simulation approach for both the longest path as well as the maximum-hops path of Fig. 8.

the paths of the mesh metro network for the typical carrier can be transparently engineered.

VII. Today's Metro Network Architectures: The Latest Case Study

The ongoing telecommunications market slowdown has inevitably affected the equipment and DWDM technology deployment scenarios in the metro area. The view of Fig. 3 with transparent interconnections of IOF and edge rings has not yet materialized. In fact any type of transparent ring interconnection is not considered realistic under the current traffic demand scenarios, with the cost of transparency proving to be prohibitive. What has happened instead has been initially a slow introduction of point-to-point DWDM as fiber relief with stacked SONET OC-48/192 collapsed rings or possible mesh connectivity among only the major hubs of metro networks. OADM capability has continued to be provided in metro networks through the use of static (nonreconfigurable) band filters with architectures similar to that shown in Fig. 5. Improvements in band and channel filters have allowed network designs to evolve to 100 GHz channel spacing, with one or no channels in the guard bands of the band filters. This has allowed system providers to offer an equivalent capacity using just the C-band, thus curbing the use of additional C/L-band splitters on day one, and the use of L-band components when the system requires an upgrade.

What is now beginning to be contemplated and expected to materialize in the 2004–2005 time frame is DWDM ring or mesh connectivity of only the major stations in the region, called superhubs, using reconfigurable OADM (R-OADMs) equipment. This future-proofing, which would allow the network provider to eliminate stranded bandwidth, potentially speed up provisioning, and provide a solution that can adequately handle forecast uncertainties, is now being investigated and deemed possible due to component cost reductions in the past 1–2 yr.

Fig. 11 shows the current deployment status and a realistic evolution scenario of a typical network in a highly populated metro region which is serviced by an ILEC [77].

All rings shown in Fig. 11 are still based on SONET/SDH equipment and the move to transparency involves only the super hubs which are being connected in a ring or a mesh connectivity pattern. In typical densely populated metropolitan areas like New York City, Philadelphia, or Atlanta, superhubs will number only a few and will typically be spaced 30 to 50 km apart with the possibility of much shorter distances. For example in the second network case study of Section VI, typical large stations (corresponding to superhubs of Fig. 11) are only 5 to 10 km apart in the central downtown sections of a major city. Superhubs generically all look the same and system integrators are currently evaluating the cost/performance tradeoffs associated with the implementation of these using the latest market technologies for reconfigurable OADMs, a glimpse of which we present below in our latest case study. The established DWDM ring or mesh topologies among superhubs are running at either OC-48 or OC-192 with current implementations occurring primarily at OC-192; OC-48 dominates for the SONET connectivity among hubs and OC-3 and OC-12 are present among the CO SONET connections.

Clearly Fig. 11 indicates that the deployment of DWDM in optical MANs is still at its initial stage despite the largely optimistic predictions of the late 90s. This is due to the low demand for wavelength-level services. The above has some major implications in terms of the way these networks are currently designed and engineered. The majority of the transport layer effects studied in our previous work and outlined in Section IV above are now much less significant since "true transparent" paths only span a few stations (superhubs only) and likely extend to maximum distances of less than 100 km. In trying to understand the main design issues and the cost versus performance tradeoffs that govern the design of today's metro networks we investigated a typical metro network case study based on the generic network design of Fig. 11 focusing on a typical major U.S. city as shown in Fig. 12. Essentially this network consists of only the all-optical part of the network of Fig. 11 (i.e., the superhubs) forming what in graph theory is called *a diameter two graph*. This essentially means that getting to any superhub from any other one requires a maximum of only

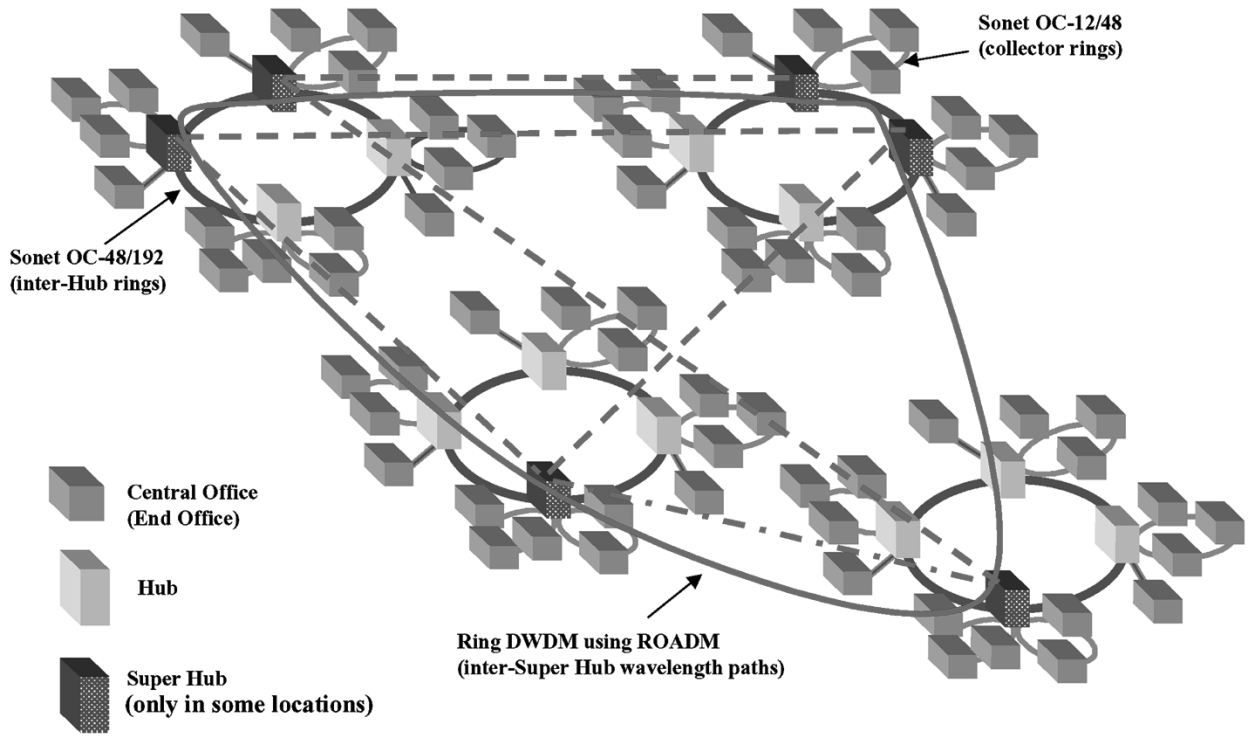

Fig. 11. Current DWDM metro network deployment scenario. All rings represent typical SONET OC-12/48/192 designs. DWDM is only deployed between the superhub nodes (dark squares) in a ring (solid) or possible mesh (dotted) configurations [77].

two all-optical hops. Employing Dijkstra's shortest path routing algorithm [78] shows that the longest optical path does not exceed 70 km. It is clear from the above observations that the worst-case paths in this network case study are much less constrained in terms of transport layer effects than the corresponding ones in the case study presented in Section VI. As a result, network engineering is simpler in terms of accounting for performance impairments and becomes an exercise on how to best take advantage of performance versus cost tradeoffs which is more of a budgeting approach as outlined in Section V (simulation step 3). We start by focusing on a connection from node A to node D. Path A-B-D is the shortest path for this connection (30 km). To provision the protection path for this connection we apply a typical diverse path routing algorithm [79], [80] that results in the path A-F-D which spans 70 km. In case of failure, the reprovisioned path will be A-C-E-F-D which is 65 km long. For the purposes of this study we focus on the worst-case path A-F-D (70 km) (Fig. 12) and try to engineer typical OC-192 services based on that. Superhubs are all considered to have similar R-OADM equipment whose basic architecture is shown in Fig. 13 for a typical 4×4 design.

The term R-OADM is used instead of the cross-connect terminology since as shown in Fig. 13 the actual number of all-optical interfaces might be small (in the above case 2 IN, 2 OUT) compared to the other transponder-based interfaces and thus the above equipment can be viewed as an all optical add/drop design with reconfigurable capabilities rather than an all-optical cross connect. The network element design of Fig. 13 will serve extremely well since the client interfaces can be the add/drops to the local CO and/or hub rings of Fig. 11. While this may not be the eventual implementation of an ROADM in a metro network, we believe it to be one that is being actively considered by several designers, and it serves as a useful starting

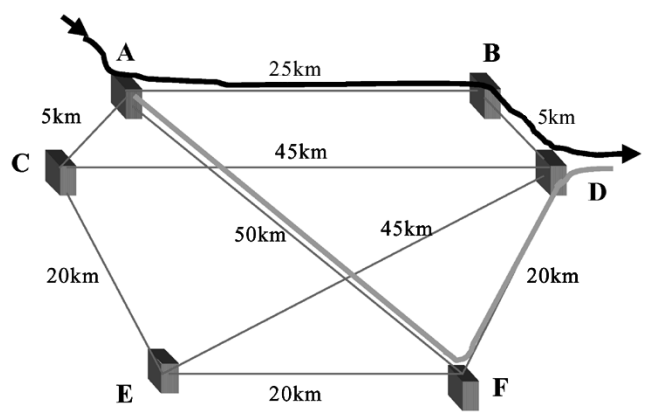

Fig. 12. DWDM metro network case study based on the current network deployment scenario of an ILEC. Nodes represent only superhub stations with typical distances (not drawn to scale) based on Fig. 11.

point for our network investigations. It is based on the B&S concept and built using couplers, amplifiers, filters, and $1 \times N$ switches. Such $1 \times N$ components that offer reconfigurability have been recently proposed [81], [82] and offer the advantage of incorporating the MUX/DMUX and switching capabilities all in one module. In [81] these were proposed as transparent switch fabrics that distribute any optical wavelength from any input port to one of four output ports (1×4) implemented with bulk optics and microelectromechanical system mirrors (MEMS). In the R-OADM design of Fig. 13, traffic from two of the input ports (1 and 2) is split into the four output ports using 1×4 splitters. Outputs 3 and 4 can selectively receive a fraction (or all) of the traffic from each fiber using $1 \times N$ splitters and tunable filters just as described in the basic B&S design of Fig. 6. In our case, 65% of the incoming traffic on each one

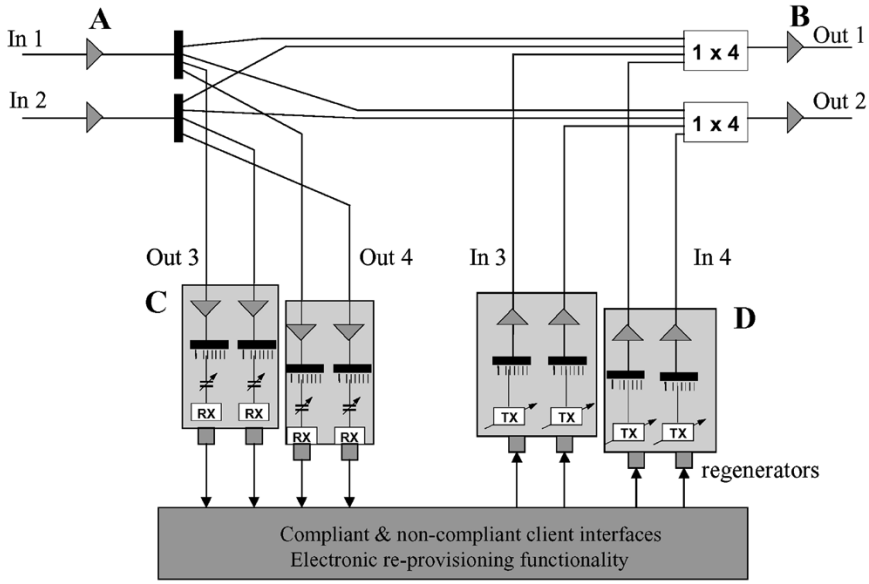

Fig. 13. Typical 4×4 ROADM based on 1×4 wavelength selective switch and B&S-type of architecture. Client interfaces (compliant: C&L band, noncompliant: 1300 nm-type) use regenerators and electronic means to achieve the reprovisioning functionality for the paths of the network of Fig. 12 A, B, C, D are metro amplifier designs.

of the input fibers (1 and 2) is assumed to be accessible which is typical of the needs of a superhub. For our case study we assumed 40 channels (195.9–192.0 THz), with 100-GHz spacing, thus access to 26 channels is assumed on each fiber at the drop side (similarly for the add side). The 1×4 selective switches on the output of the design provide the switching, equalization and blocking capabilities as described in previous sections. Insertion loss of about 5 dB and in-band crosstalk of about -50 dB [81] [Fig. 4(b)] where demonstrated for the 1×4 s and are thus used in our simulation models. In trying to engineer the worst-case path of Fig. 12 effects like filter concatenation, crosstalk and nonlinearities will have significantly less magnitude than in the previous case studies. The number of optical filters through which the signal passes is now only three which is based on the work presented in [83] results in negligible penalty. Incoherent common channel crosstalk penalty is budgeted at only 0.5 dBQ based on the model presented in Section IV, information from [64, Fig. 12] and the individual 1×4 specifications given above [81]. Fiber nonlinearities are almost negligible for the channel spacing, bit rate, and per-channel launched power in this case ($+1$ dBm/channel) and are budgeted at 0.1 dBQ. PMD is budgeted at 0.2 dBQ based on the analytical model presented in [64] and references therein and PDL, PMD/PDL interactions are ignored based on results from previous work on the subject [68] and the fact that the number of optical components that the signal traverses before being regenerated is rather small. A safety margin of 1 dBQ is allocated for component aging and factored into the budgeting model. In designing the amplifiers A,B,C, and D of Fig. 13 cost versus performance tradeoffs are taken into account. Amplifier A is a more expensive two-coil design equipped with internal VOAs for variable gain operation. By incorporating the VOA loss inside the amplifier as opposed to having it outside integrates functionalities and achieves variable span lengths at lower power and cost [84]. A total of 19-dBm output power is achieved with gains in the 20-dB range and a noise figure of about 6 dB. For amplifiers B and D cheaper single-coil designs are used with total output power about 13 dBm and gains of around 10 dB and higher noise figures (9 dB). Amplifier C is not needed in the particular implementations of Fig. 13. In our case study for the first simulation run, we use DML transmitters and typical dispersion compensation modules (placed midstage at the amplifier sites) to account for the dispersion of the standard single-mode fiber of the path A-F-D in the network of Fig. 12. DMLs operating at OC-48 speeds have been the driving force for metro system implementations for a while. At OC-192 however, their large chirp has traditionally prevented their use except from implementations over specialized fiber [85]. Recently DML commercial products at OC-192 rates have emerged that are very low cost and prove suitable for the applications we have been discussing [86]. However, the sizes of networks that such devices can support are quite restricted. More recently, electronic dispersion compensation (EDC) technologies have been showing significant momentum due to their potential cost effectiveness [87]. Previous work has demonstrated the effectiveness of EDC in systems based on EA modulators [88] and more recently in the case of $LiNbO_3$ external modulators [89] where it was shown that such technology can provide 30%–40% improvement compared to the typical dispersion-limited reach of such transmitters. In Feuer *et al.* [90] substantial enhancement of maximum transmission distance is shown using a combination of DML transmitters and EDC at the receiver. Based on our setup described earlier, the second simulation run adds EDCs at the receiver of path A-F-D of Fig. 12 and engineers all 40 possible channels through it. Fig. 14 presents the results for the two simulation runs described above. In the case where EDCs are used at the receiver a phenomenological model for the EDC is used in our simulation procedure. This simple model is derived from [90, Fig. 5] where the penalty is presented versus single mode fiber span length (i.e., dispersion for a channel). Specifically, the residual dispersion (after the optical dispersion compensation is applied) for every channel in our network is monitored and the

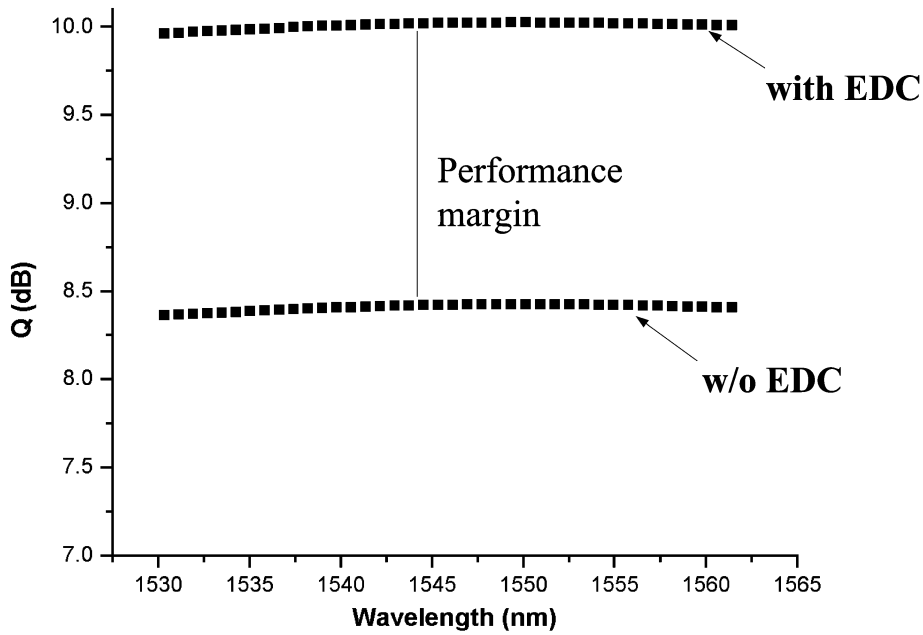

Fig. 14. Simulation results for the engineering of path A-F-D of Fig. 12 using DML transmitters at OC-192 rate, dispersion compensation modules for typical single-mode fiber dispersion compensation, and (a) no EDC; (b) with EDCs. EDC model uses dispersion penalty versus span length graph as described in [90].

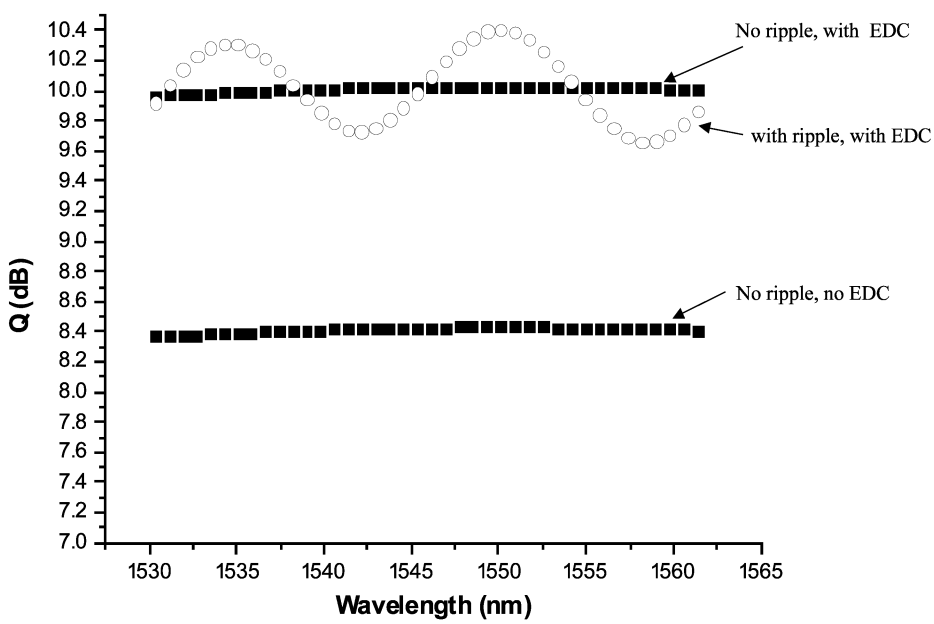

Fig. 15. Performance tradeoffs between the use of EDC and components with relaxed performance specifications.

penalty that results with the use of EDC is read from the above graph in [90]. This penalty is used in the budgeting procedure described above as the dispersion/chirp impairment. It is clear from [90, Fig. 5] that in the case where DMLs are used supported distances even with the use of EDCs can not expand beyond 20 kms. As a result, in our case study EDCs are used in addition to basic optical dispersion compensation modules (no dispersion slope compensation) to deal with the residual dispersion at each channel. The derivation of a more elaborate simulation model for the EDC is currently underway and will be presented in a future work. Clearly, EDC solutions can not substitute in-line dispersion compensation units, however they provide significant performance improvements when used to account for residual dispersion in the path. In our case study, a performance margin of 1.6 dBQ can be achieved as shown in Fig. 14. This could be allocated to mitigate other impairments such as PMD which in existing designs over older fiber can be significant. However, in our case study, all impairments are small and a *green-field* network scenario is assumed. Another cost-effective consequence of the use of EDCs is the ability to use this performance margin to relax specifications on individual components. An example would be ripple of amplifiers, and/or other optical components as shown in Fig. 15 where a ripple of 0.5 dB per amplifier and 0.1 dB per component is assumed. For illustration purposes only, the ripple is assumed to be systematic, sinusoidal in shape, but rather conservative in its value. It is clear from Fig. 15 that there is still enough margin for components with worse performance and thus less costly to

manufacture (until the required 8.5 dB for BER $< 10^{-12}$ is reached). Amplifier ripples of 0.75–1 dB can be common for low-cost metro designs.

Eventually, however, the widespread use of techniques such as EDC and forward error correction (FEC) to enable a larger margin in metro systems, and therefore lower cost in other components, or increase the reach using existing components, will be driven through economic tradeoffs. EDC and FEC techniques may allow a lower first-installed cost since they are based upon a channel-by-channel implementation, but this needs to be studied further and is a subject of our future work.

VIII. Conclusion

This paper summarizes our work on design and engineering of the transport layer of metropolitan optical networks. Several network case studies were simulated that clearly demonstrated the metro network architecture evolution trends during the last few years. The current telecommunications slowdown had a significant impact on the advancement of WDM in metro and in particular it affected how the currently implemented architectures are engineered. It is clear that some of the major performance impairments which we were concerned with in the past have no significant impact in today's deployed scenarios mainly because the truly transparent paths are much shorter and traverse fewer components than originally studied. On the center stage are the performance versus cost tradeoffs which lead to the use of new and cheap technologies such as 10 Gb/s DMLs, electronic dispersion compensators and possibly others. A direct consequence of the above is the use of cheaper components and increased performance margins that can avoid worst-case engineering designs.

References

[1] G. Hill, P. Chidgey, F. Kaufhold, T. Lynch, O. Sahlen, M. Gustavsson, M. Janson, B. Lagerstrom, G. Grasso, F. Meli, S. Johansson, J. Ingers, L. Fernandez, S. Rotolo, A. Antonielli, S. Tebaldini, E. Vezzoni, R. Caddedu, N. Caponio, F. Testa, A. Scavennec, M. Mahony, J. Zhou, A. Yu, W. Sohler, U. Rust, and H. Hermann, "A transport network layer based on optical network elements," *J. Lightwave Technol.*, vol. 11, pp. 667–679, May/June 1993.

[2] C. A. Brackett, A. Acampora, J. Sweitzer, G. Tangonan, M. Smith, W. Lennon, K. Wang, and R. Hobbs, "A scalable multiwavelength multihop optical network: A proposal for research on all-optical networks," *J. Lightwave Technol.*, vol. 11, pp. 736–753, May/June 1993.

[3] S. B. Alexander, R. Bondurant, D. Byrne, V. Chan, S. Finn, R. Gallager, B. Glance, H. Haus, P. Humblet, R. Jain, I. Kaminow, M. Karol, R. Kennedy, A. Kirby, H. Le, A. Saleh, B. Schofield, J. Shapiro, N. Shankaranarayanan, R. Thomas, R. Williamson, and R. Wilson, "A precompetitive consortium on wide-band all-optical networks," *J. Lightwave Technol.*, vol. 11, pp. 714–735, May/June 1993.

[4] R. E. Wagner, R. Alferness, A. Saleh, and M. Goodman, "MONET: Mulriwavelength optical networking," *J. Lightwave Technol.*, vol. 14, pp. 1349–1355, June 1996.

[5] C. A. Brackett, "Is there an emerging consensus on WDM networking," *J. Lightwave Technol.*, vol. 14, pp. 936–941, June 1996.

[6] A. M. Saleh and J. M. Simmons, "Architectural principles of optical regional and metropolitan access networks," *J. Lightwave Technol.*, vol. 17, pp. 2431–2448, 1999.

[7] N. Ghani, J.-Y. Pan, and X. Cheng, *Optical Fiber Telecommunications*. San Diego, CA: Academic, 2002, vol. IV-B, ch. 8.

[8] F. Farjady, N. Antoniades, and M. J. Yadlowsky, "Value of fiber overlays in WDM metro networks," *IEEE Photon. Technol. Lett.*, vol. 15, pp. 329–333, Feb. 2003.

[9] N. Antoniades, M. Yadlowsky, and V. L. daSilva, "Computer simulation of a metro WDM ring network," *IEEE Photon. Technol. Lett.*, vol. 12, no. 11, pp. 1576–1578, Nov. 2000.

[10] Y. Chen *et al.*, "Metro optical networking," *Bell Labs Tech. J.*, vol. 4, no. 1, pp. 163–186, Jan.–Mar. 1999.

[11] N. A. Jackman *et al.*, "Optical cross connects for optical networking," *Bell Labs Tech. J.*, vol. 4, no. 1, pp. 262–281, Jan.–Mar. 1999.

[12] N. Antoniades, A. Boskovic, J. Downie, N. Madamopoulos, D. Pastel, J.-K. Rhee, and M. Yadlowsky, "Engineering the performance of DWDM metro networks," in *NFOEC 2000 Conf. Tech. Dig.*, Denver, CO, Aug. 2000, pp. 204–211. Session B2.

[13] L. Nederlof *et al.*, "Value proposition for configurable optical network elements," in Opt. Fiber Commun. Conf. (OFC) 2001, Anaheim, CA, Mar. 2001.

[14] G. Ellinas *et al.*, "Architecture considerations in merging multi-vendor WDM rings for the MONET Washington D.C. network," in Opt. Fiber Commun. Conf. (OFC) 1999, San Diego, CA, Feb. 1999.

[15] O. Gerstel and R. Ramaswami, "Upgrading SONET rings with WDM instead of TDM: An economic analysis," in Opt. Fiber Commun. Conf. (OFC) 1999, San Diego, CA, Feb. 1999.

[16] M. Simcoe, "A layered architecture for metro optical networks," in *NFOEC 2000 Conf. Tech. Dig.*, Denver, CO, Aug. 2000, pp. 602–610. Session D4.

[17] P. Humblet, "The direction of optical technology in the metro area," in *Opt. Fiber Commun. Conf. (OFC) 2001*, Anaheim, CA, Mar. 2001, pp. WBB1-1–WBB1-3.

[18] P. Wong, "Network architectures in the metro DWDM environment," in *NFOEC 2000 Conf. Tech. Dig.*, Denver, CO, Aug. 2000, pp. 588–596. Session D4.

[19] P. Bonenfant and A. Moral, "Optical data networking," *IEEE Commun. Mag.*, vol. 38, pp. 63–70, Mar. 2000.

[20] K. Bala, "WDM optical network architectures for a data-centric environment," in NFOEC 2000 Conf. Tech. Dig., Orlando, FL, Sept. 1998.

[21] I. Tomkos, R. Hesse, N. Madamopoulos, C. Friedman, N. Antoniades, B. Hallock, R. Vodhanel, and A. Boskovic, "Transport performance of an 80-Gb/s WDM regional area transparent network utilizing directly modulated lasers," *J. Lightwave Technol.*, vol. 20, pp. 562–573, Apr. 2002.

[22] L. Berthelon *et al.*, "Managed, 2R-regenerated transparent optical networking field trial spanning core and access," in *Opt. Fiber Commun. Conf. (OFC) 2001*, Anaheim, CA, Mar. 2001, pp. WN1-1–WN1-3.

[23] I. White *et al.*, "Experimental demonstration of the HORNET survivable bi-directional ring architecture," in *Opt. Fiber Commun. Conf. (OFC) 2002*, Anaheim, CA, Mar. 2002, pp. 346–348. paper WW1.

[24] N. Takachio *et al.*, "12.5-GHz-spaced super dense WDM ring network handling 256 wavelengths with tapped-type OADMs," in *Opt. Fiber Commun. Conf. (OFC) 2002*, Anaheim, CA, Mar. 2002, pp. 349–350. paper WW2.

[25] H. D. Kim *et al.*, "Demonstration of bi-directional WDM network," in *Proc. Opt. Fiber Commun. Conf. (OFC) 2002*, Anaheim, CA, Mar. 2002, pp. 353–355. paper WW5.

[26] L. Noirie *et al.*, "32 × 10 Gbit/s DWDM metropolitan network demonstration with 10 waveband-ADM's and 155 km TeraLight™ metro fiber," in *Proc. Opt. Fiber Commun. Conf. (OFC) 2002*, Anaheim, CA, Mar. 2002, pp. 442–443. paper TH4.

[27] K. C. Reichmann *et al.*, "An eight-wavelength 160-km transparent metro WDM ring network featuring cascaded erbium-doped waveguide amplifiers," *IEEE Photon. Technol. Lett.*, vol. 13, pp. 1130–1132, Oct. 2001.

[28] A. Richter *et al.*, "Germany-wide DWDM field trial: Transparent connection of a long-haul link and a multi-channel metro network," in *Opt. Fiber Commun. Conf. (OFC) 2002*, Anaheim, CA, Mar. 2002, pp. 442–443. paper TH4.

[29] K. Noguchi *et al.*, "The first field trial of a wavelength routing WDM full-mesh network system (AWG-STAR) in a metropolitan/local area," in *Proc. Opt. Fiber Commun. Conf. (OFC) 2003*, Atlanta, GA, Mar. 2003, pp. 611–613. paper THAA5.

[30] P. Toliver *et al.*, "Experimental field trial of waveband switching and transmission in a transparent reconfigurable optical network," in *Proc. Opt. Fiber Commun. Conf. (OFC) 2002*, Atlanta, GA, Mar. 2003, pp. 783–784. paper FR1.

[31] Press Release (2002, May 28). [Online]. Available: http://www.photuris.com/2003/news/pr/2002_0528.shtml

[32] ONLINE Family of Metro Products [Online]. Available: http://www.ciena.com/products/metro/metronetworking.htm

[33] A. Boskovic, M. Sharma, N. Antoniades, and M. Lee, "Broadcast and select OADM nodes: Application and performance tradeoffs," in *Proc. Optical Fiber Communication Conf. (OFC'02)*, Anaheim, CA, Mar. 15–21, 2002, pp. 158–159. paper TuX2.

[34] Press Release (2003, May). [Online]. Available: http://www.opvista.com/

[35] Rsoft Design Group [Online]. Available: http://www.rsoftdesign.com/

[36] VPIsystems, Inc. [Online]. Available: http://www.vpiphotonics.com/

[37] Optiwave, Inc. [Online]. Available: http://www.optiwave.com

[38] I. Tomkos, M. Vasilyev, J.-K. Rhee, M. Mehendale, S. Tsuda, B. Szalabofka, and B. Hallock, "80 × 10.7 Gb/s ultra-long-haul (4200 km) DWDM network with dynamic operation of broadcast & Select reconfigurable OADMs," presented at the Optical Fiber Communication Conf. (OFC'02), Anaheim, CA, 2002. postdeadline paper.

[39] R. Vodhanel *et al.*, "National scale WDM networking demonstration by the MONET consortium," presented at the Optical Fiber Communication Conf. (OFC'97), Dallas, TX, 1997, postdeadline paper PD 27-1.

[40] W. T. Anderson, "The MONET project final report," in *Proc. IEEE/OSA Opt. Fiber Commun. Conf.*, Baltimore, MD, Feb. 2000, pp. 148–149. paper WJ1-1.

[41] A. F. Elrefaie, *Proc. ICC'93*, Geneva, Switzerland, May 23–26, 1993, pp. 1245–1251. paper 48.7.

[42] W. Goralski, *SONET/SDH*, 3rd ed. New York: McGraw Hill, 2002.

[43] A. F. Elrefaie, *Proc. Optical Fiber Communication Conf. (OFC'92)*, San Jose, CA, Feb. 2–7, 1992, pp. 255–256.

[44] A. Dwivedi and R. E. Wagner, "Traffic model for USA long-distance optical network," in *Proc. IEEE/OSA Opt. Fiber Commun. Conf.*, Baltimore, MD, Feb. 2000, pp. 156–158. paper TuK11.

[45] D. Cooperson, "Short-haul WDM/optical networking: Is it (finally) for real?," in *NFOEC 2000 Conf. Tech. Dig.*, Denver, CO, Aug. 2000, pp. 530–540. Session B4.

[46] Nortel Networks, Optical Metro [Online]. Available: http://www.nortelnetworks.com/products/01/optera/metro/msp/5000/

[47] N. Antoniades, I. Roudas, R. E. Wagner, and S. F. Habiby, "Simulation of ASE noise accumulation in a wavelength add-drop multiplexer (WADM) cascade," *IEEE Photon. Technol. Lett.*, vol. 9, pp. 1274–1276, Sept. 1997.

[48] Nortel Networks, Optera Products. [Online]. Available: http://a1648.g.akamai.net/7/1648/5107/20 030 925 230 042 /www.nortelnetworks.com/products/01/optera/metro/msp/5000/collateral/56 027.13-0207-03.pdf

[49] A. Dwivedi, M. Sharma, J. Grochocinski, and R. Wagner, "Value of reach extension in long-distance networks," in *NFOEC 2000 Conf. Tech. Dig.*, Denver, CO, Aug. 2000, pp. 351–357. Session B8.

[50] A. Ranalli *et al.*, "Liquid crystal based wavelength selectable crossconnect," in *Proc. Eur. Conf. Optical Communication (ECOC)*, 1999, pp. 68–69.

[51] Avanex, Inc. Product Catalog [Online]. Available: http://www.avanex.com/products/datasheets/amplification/d0015_b.pwrequalizer_dgev3.pdf

[52] B. Bacque and D. Oprea, "R-OADM architecture: Now you can control the light," *Tropic Networks*, 2003. white paper.

[53] Press Release (2003, May). [Online]. Available: http://www.opvista.com/

[54] I. Roudas, N. Antoniades, D. H. Richards, R. E. Wagner, J. L. Jackel, S. F. Habiby, T. E. Stern, and A. F. Elrefaie, "Wavelength-domain simulation of multiwavelength optical networks," *IEEE J. Select. Topics Quantum Electron.—Special Issue on Modeling of High Data Rate Optical Fiber Communications Systems (*Invited Paper*)*, vol. 6, pp. 348–362, Mar./Apr. 2000.

[55] I. Roudas, D. H. Richards, N. Antoniades, J. L. Jackel, and R. E. Wagner, "An efficient simulation model of the erbium-doped fiber for the study of multiwavelength optical networks," *Opt. Fiber Technol. (*Invited Paper*)*, vol. 5, pp. 363–389, Oct. 1999.

[56] A. F. Elrefaie, R. E. Wagner, D. Atlas, and D. G. Daut, "Chromatic dispersion limitations in coherent lightwave transmission systems," *J. Lightwave Technol.*, vol. LT-6, pp. 704–709, May 1988.

[57] P. J. Corvini and T. L. Koch, "Computer simulation of high bit rate optical fiber transmission using single frequency lasers," *J. Lightwave Technol.*, vol. LT-5, pp. 1591–1595, Nov. 1987.

[58] J. C. Cartledge and G. S. Burley, "The effect of laser chirping on lightwave system performance," *J. Lightwave Technol.*, vol. 7, pp. 568–573, Mar. 1989.

[59] J. C. Cartledge and A. F. Elrefaie, "Effect of chirping-induced waveform distortion on the performance of direct detection receivers using traveling-wave semiconductor optical amplifiers," *J. Lightwave Technol.*, vol. 9, pp. 209–219, Feb. 1991.

[60] C. S. Li, F. F. K. Tong, K. Liu, and D. G. Messerschmitt, "Channel capacity optimization of chirp-limited dense WDM/WDMA systems using OOK/FSK modulation and optical filters," *J. Lightwave Technol.*, vol. 10, pp. 1148–1161, Aug. 1992.

[61] K. Hinton and T. Stephens, "Modeling high-speed optical transmission systems," *IEEE J. Select. Areas Commun.*, vol. 11, pp. 380–392, Apr. 1993.

[62] L. Koch and R. A. Linke, "Effect of nonlinear gain reduction on semiconductor laser wavelength chirping," *Appl. Phys. Lett.*, vol. 48, pp. 613–615, Mar. 1986.

[63] T. L. Koch and J. E. Bowers, "Nature of wavelength chirping in directly modulated semiconductor lasers," *Electron. Lett.*, vol. 20, pp. 1038–1039, Dec. 1984.

[64] N. Antoniades, A. Boskovic, I. Tomkos, N. Madamopoulos, M. Lee, I. Roudas, D. Pastel, M. Sharma, and M. Yadlowsky, "Performance engineering and topological design of metro WDM optical networks," *IEEE J. Select. Areas Commun. (Special Issue on WDM Based Optical Networks)*, vol. 20, pp. 149–165, Jan. 2002.

[65] I. Roudas, N. Antoniades, T. Otani, T. E. Stern, R. E. Wagner, and D. Q. Chowdhury, "Accurate modeling of optical multiplexers/demultiplexers concatenation in multiwavelength optical networks," *J. Lightwave Technol.*, vol. 20, pp. 921–936, June 2002.

[66] K. P. Ho, "Analysis of homodyne crosstalk in optical networks using Gram–Charlier series," *J. Lightwave Technol.*, vol. 17, pp. 149–153, 1999.

[67] T. Kamalakis, T. Sphicopoulos, and M. Sagriotis, "Accurate estimation of the error probability in the presence of in-band crosstalk noise in WDM networks," *J. Lightwave Technol.*, vol. 21, pp. 2172–2181, Oct. 2003.

[68] M. Lee, N. Antoniades, and A. Boskovic, "PDL-induced channel power divergence in a metro WDM network," *IEEE Photon. Technol. Lett.*, vol. 14, pp. 561–563, Apr. 2002.

[69] B. Ramamurthy, D. Datta, H. Feng, J. Heritage, and B. Mukherjee, "Impact of transmission impairments on the telegraphic performance of wavelength-routed optical networks," *J. Lightwave Technol.*, vol. 17, pp. 1713–1723, Oct. 1999.

[70] M. D. Vaughn and R. E. Wagner, "Metropolitan network traffic demand study," in *IEEE/LEOS Annual Meeting, Tech. Dig. 2000*, Piscataway, NJ, Nov. 13–16, 2000. MK4, IEEE/LEOS.

[71] N. Madamopoulos, M. D. Vaughn, L. Nederlof, and R. E. Wagner, "Metro network architecture scenarios, equipment requirements and implications for carriers," in *Opt. Fiber Commun. Conf. (OFC), Tech. Dig. 2001*, Anaheim, CA, Mar. 17–22, 2001. WL2.

[72] A. Dwivedi, "Optical networking," in *NCF, Tech. Dig. 1999*, Chicago, IL, Oct. 25–28, 1999.

[73] M. C. Jeruchim, P. Balaban, and K. S. Shanmugan, *Simulation of Communication Systems*. New York: Plenum, 1992.

[74] G. P. Agrawal, *Fiber-Optic Communication Systems*. New York: Wiley-Interscience, 1997.

[75] I. Tomkos, R. Hesse, N. Antoniades, and A. Boskovic, "Impact of filter concatenation effects on the performance of metropolitan area optical networks utilizing directly modulated lasers," in *Proc. Optical Fiber Communication Conf. (OFC'01)*, Anaheim, CA, Mar. 2001, pp. BB4.1–BB4.3. OSA.

[76] N. Madamopoulos, N. Antoniades, I. Roudas, M. Vaughn, and R. E. Wagner, "Design, transport performance study and engineering of a 11 Tb/s US metro network," in *Proc. Optical Fiber Commun. Conf. (OFC'02)* , Anaheim, CA, Mar. 15–21, 2002, pp. 444–445. OSA, paper ThH6.

[77] S. Elby. (2002, Oct.) Public Network Reliability and Resiliency. Columbia Univ. [Online]. Available: http://www2.cvn.columbia.edu/course/elene6901/session/S.ElbyNetworkReliabilityTalkPT1.ppt

[78] R. E. Tarjan, *Data Structures and Network Algorithms*. Philadeplhia, PA: SIAM, 1983.

[79] J. W. Suurballe, "Disjoint paths in a network," *Networks*, vol. 4, pp. 125–145, 1974.

[80] R. Bhandari, *Survivable Networks: Algorithms for Diverse Routing*. Norwell, MA: Kluwer Academic, 1999.

[81] D. Marom, D. Nelson, D. Greywall, N. Basavanhally, P. Kolodner, Y. Low, P. C. Bolle, S. Chandrasekhar, L. Buhl, and C. Giles, "Wavelength-selective 1 × 4 switch for 128 WDM channels at 50 GHz spacing," presented at the Optical Fiber Commun. Conf. (OFC) 2002, Anaheim, CA, Mar. 2002. Postdeadline paper FB7-1.

[82] C. Doerr, L. Stulz, D. Levy, L. Gomez, M. Capuzzo, J. Bailey, R. Long, A. Wong-Foy, E. Laskowski, E. Chen, S. Patel, and T. Murphy, "Eight wavelength add-drop filter with true reconfigurability," *IEEE Photon. Technol. Lett.*, vol. 15, pp. 138–140, Jan. 2003.

[83] J. Downie and A. Ruffin, "Analysis of signal distortion and crosstalk penalties induced by optical filters in optical networks," *J. Lightwave Technol.*, vol. 21, pp. 1876–1886, Sept. 2003.

[84] K. Wundke, "Advanced amplifier design: Physics and system limitations," in *Proc. Optical Fiber Communication Conf. (OFC' 03)*, Atlanta, GA, 2003. Paper WK1.

[85] I. Tomkos, B. Hallock, I. Roudas, R. Hesse, A. Boskovic, J. Nakano, and R. Vodhanel, "10-Gb/s transmission of 1.55-mm directly modulated signal over 100 km of negative dispersion fiber," *IEEE Photon. Technol. Lett.*, vol. 13, pp. 735–737, July 2001.

[86] Lightwave Online [Online]. Available: http://lw.pennnet.com/Articles/Article_Display.cfm?Section=OnlineArticles&SubSection=Display&PUBLICATION_ID=13&ARTICLE_ID=194 453&pc=ENL

[87] *Optical Fiber Telecommunications*. San Diego, CA: Academic, 2002, vol. IV-B, ch. 14.

[88] S. Woodward, M. Feuer, S. Huang, and M. Boroditsky, "Demonstration of an electronic dispersion compensator in a 100 km, 10 Gb/s ring network," *IEEE Photon. Technol. Lett.*, vol. 15, pp. 867–869, June 2003.

[89] L. Paraschis, "Optical technology innovation in metropolitan networks," in *Optical Networking II Conf. (*Keynote Invited Paper*)*, 2003. , SPIE, 5282-01, APOC.

[90] M. Feuer, S. Huang, S. Woodward, O. Coskun, and M. Boroditsky, "Electronic dispersion compensation for a 10-Gb/s link using a directly modulated laser," *IEEE Photon. Technol. Lett.*, vol. 15, pp. 1788–1790, Dec. 2003.

[91] Vendors Race for Reconfigurability (2004, Feb. 26). [Online]. Available: www.lightreading.com

N. Antoniades (S'91–M'92) received the B.S., M.S., M.Phil., and Ph.D. degrees, all in electrical engineering, from Columbia University, New York, in 1992, 1993, 1996, and 1998, respectively. His Ph.D. research focused on the modeling of optical components and fiber-optic communication systems and networks.

He was with Bellcore (currently Telcordia Technologies), Red Bank, NJ, from 1994 to 1998, where he helped in the construction of the first experimental prototype multiwavelength optical networks (MONET and ONTC) based on large-scale U.S. government-supported research projects. From 1998 to summer 2002, he was a Senior Research Scientist at the Photonic Research & Test Center, Corning, Inc., Somerset, NJ. His activities included the design, engineering, and prototyping support of novel wavelength-division-multiplexing solutions for the regional and metro optical networking space, product techno/economic value propositions for next-generation optical devices and network elements, customer technical support, the modeling of transmission impairments, and research on new modeling techniques for optical systems and networks. From September 2002 until April 2003, he was a Visiting Researcher at Columbia University, where he participated in research on resilient telecommunication networks and was involved in the activities of the newly created center for resilient networks. At the same time, he worked for 3NE Solutions, New York, as a Marketing Engineer supporting a number of client accounts on market-driven development, product value analysis, engineering, and customer technical support focusing in the field of bio-engineering and wireless telecommunications. Since May 2003, he has been an Assistant Professor of Electrical Engineering at the Engineering Science and Physics Department of The College of Staten Island, The City University of New York. He is currently teaching and conducting research in the area of telecommunications. One of his research activities focuses on designing the high-capacity next-generation fiber-optic systems that will support the next-generation Internet and its high-bandwidth demand applications of the near future. At the same time, he is interacting with various telecommunications research laboratories in the area and works on practical problems that the typical telecom companies will be facing as they deploy their modern fiber-optic equipment in the field. Another area of his research focuses on designing telecommunication networks involving various technologies (wireless, fiber optic, and satellite) that will ensure "resilient," i.e., robust, operation during times of major disasters. He has published more than 50 manuscripts in all leading journals and conferences. He currently holds two U.S. patents in the field of telecommunications with three others submitted and pending.

Dr. Antoniades is a Member of the IEEE Lasers & Electro-Optics Society (LEOS) and the LEOS annual conference committee on Optical Networks and Systems and a Committee Member for Optical Networks for the Optical Fiber Communications conference.

I. Roudas received the B.S. degree in physics and the M.S. degree in electronics and radio engineering from the University of Athens, Athens, Greece, in 1988 and 1990, respectively, and the M.S. degree in components and devices of optical and microwave communications and the Ph.D. degree in coherent optical communication systems from the École Nationale Supérieure des Télécommunications, Paris, France, in 1991 and 1995, respectively.

From 1995 to 1998, he was with the Optical Networking Research Department, Bell Communications Research (Bellcore), Red Bank, NJ. In addition, he was an Adjunct Professor of the graduate course entitled Lightwave Systems with the Electrical Engineering Department, Columbia University, New York, during fall 1997 and 1998. From 1999 to 2002, he was with the Photonic Research and Test Center, Corning, Inc., Somerset, NJ. He is currently with the Department of Electrical and Computer Engineering, University of Patras, Patras, Greece, as an Associate Professor of optical communications. He is the author or coauthor of more than 45 papers in scientific journals and international conferences and holds one patent. His research interests include polarization-mode dispersion compensation, electronic-dispersion compensation, advanced modulation formats, and forward-error correction.

Dr. Roudas serves as a Reviewer for the JOURNAL OF LIGHTWAVE TECHNOLOGY, the IEEE PHOTONICS TECHNOLOGY LETTERS, and *Optics Communications*.

G. Ellinas (S'90–M'91) received the B.S., M.S., and Ph.D. degrees in electrical engineering from Columbia University, New York.

He was formerly a Senior Network Architect at Tellium, Inc., where he worked on lightpath provisioning and fault restoration algorithms in optical mesh networks and the architecture design of the microelectromechanical-systems-based all-optical switch. He also served as a Senior Research Scientist with the Optical Networking Research Group of Telcordia Technologies' (formerly Bellcore). From 1993 to 2000, he conducted research for the Optical Networks Technology Consortium (ONTC), the Multiwavelength Optical Networking (MONET), and the Next Generation Internet (NGI) projects. He also served as an Adjunct Assistant Professor at Columbia University and the University of Maryland, teaching courses on multiwavelength optical networking in 1999 and 2000, respectively. He is currently an Associate Professor of Electrical Engineering at City College, The City University of New York. He has authored and coauthored more than 60 journal and conference papers, is the holder of 17 patents on optical networking, and has more than 10 U.S. and international patent applications currently pending. His research interests are in the areas of optical architectures, routing and wavelength assignment algorithms, fault protection/restoration techniques in arbitrary mesh optical networks, and burst/packet switching in multiwavelength optical networks.

Dr. Ellinas was awarded a Fulbright fellowship from 1987 to 1991 for undergraduate studies at Columbia University

J. Amin received the M.Sc. degree in optoelectronics and laser physics from the University of Glasgow, Glasgow, U.K., in 1992 and the Ph.D. degree in optoelectronics from the University of Southampton, Southampton, U.K., in 1996.

He held a Guest Researcher position at NIST, Boulder, CO, from 1996 to 1997, working on integrated optic lasers and amplifiers and QPM devices in lithium niobate. He joined Corning, Inc., in 1997, working on research and development of novel fiber and planar waveguide devices for telecommunications applications. He moved into the Corning Photonics business unit in 1998, assuming the position of Manager of New Product Development and Customer Engineering for Photonics Components, followed by Business Manager, Integrated Optics. In 2001, he was appointed Director of Technical and Strategic Marketing for Corning Photonics. Upon the divestiture of Corning Photonics to Avanex, Inc., Painted Post, NY, he held the position of Senior Director of Strategic Marketing and Senior Product Line Director of Multiplexing and Signal Processing between August 2003 and May 2004. He returned to Corning in June 2004, where he is currently Director of Commercial Technology for the Specialty Materials group. He is an author or coauthor of more than 40 publications in the fields of optoelectronics and optical communications.